Univerzita Karlova
Přírodovědecká fakulta

Studijní program: Biologie

Studijní obor: Genetika, molekulární biologie a virologie

Darya Kuzmenko

Role coilinu při kontrole kvality snRNP částic

The role of coilin in snRNP quality control

Diplomová práce

Školitel: Assoc. Prof. David Staněk, Ph.D.

Prague, 2022

I declare that I carried out this master thesis independently, and only with the cited sources, literature and other professional sources. It has not been used to obtain another or the same degree.

Prohlašuji, že jsem závěrečnou práci zpracovala samostatně a že jsem uvedla všechny použité informační zdroje a literaturu. Tato práce ani její podstatná část nebyla předložena k získání jiného nebo stejného akademického titulu.

In/V .... date/dne ....

Author's signature/Podpis

i

Abstract: Mammalian genes are transcribed as precursors – pre-mRNA. They contain coding sequences (exons) and non-coding sequences (introns). Splicing, a process of cutting out introns and joining exons to generate mature mRNA, is carried out by a spliceosome. The spliceosome consists of five small nuclear ribonucleoprotein (snRNP) particles and numerous associated proteins. Its assembly is a complex process involving a specific nuclear sub-compartment, the Cajal body (CB). Here, we investigate function of the CB scaffold protein, coilin, in snRNP quality control in HeLa cells. Sequestration of immature snRNP in coilin-deficient cells is analysed by fluorescence *in situ* hybridisation. We show that without coilin the cells are unable to sequester them. Next, we provide evidence that absence of coilin does not sensitise HeLa cells for perturbation in snRNP maturation in terms of cell proliferation. Moreover, coilin deficiency does not result in significant changes in U4, U5 or U6 snRNA steady state levels. Therefore, coilin, and, in this way, Cajal bodies do not become essential under the conditions of strained snRNP biogenesis.

Abstrakt: Savčí geny jsou transkribovány ve formě prekurzorů – pre-mRNA. Obsahují kódující sekvence (exony) a nekódující sekvence (introny). Sestřih, proces odstranění intronů a spojení exonů za účelem vytvoření zralé mRNA, se provádí pomocí spliceosomu. Spliceosom se skládá z pěti malých jaderných ribonukleoproteinových (snRNP) částic a četných asociovaných proteinů. Jeho skládání je složitým procesem, kterého se učástní specifický jaderný subkompartment, Cajalovo tělísko (CB). V této práci zkoumáme funkci CB scaffoldového proteinu, coilinu, při kontrole kvality snRNP v HeLa buňkách. Sekvestrace nehotových snRNP částic v buňkách bez coilinu je analyzována pomocí fluorescenční *in situ* hybridizace. Ukazujeme, že buňky bez coilinu nejsou schopny nehotové snRNP částice zachytit. Dále, poskytujeme důkazy, že nepřítomnost coilinu nezvyšuje citlivost HeLa buněk vůči defektům ve zrání snRNP částic z hlediska buněčné proliferace. Navíc, nedostatek coilinu nevede k významným změnám hladin U4, U5 nebo U6 snRNA. Proto se coilin, a tudíž ani Cajalova tělíska, nestávají nezbytnými v podmínkách defektní biogeneze snRNP částic.

Klíčová slova: coilinový knockout, skládání sestřihového komplexu, nehotové snRNP částice, PRPF6

Contents

List of abbreviations

Brr	bad response to refrigeration
BS	branch site
CB	Cajal body
CBP	cap-binding protein
cDNA	complementary DNA
CRM	chromosomal maintenance
CTD	carboxy-terminal domain
DAPI	4′,6-diamidino-2-phenylindole
DSE	distal sequence element
FISH	fluorescence in situ hybridization
GAPDH	glyceraldehyde 3-phosphate dehydrogenase
GEMIN	gem-associated protein
hCINAP	human coilin-interacting nuclear ATPase protein
IR	infrared
KD	knockdown
KO	knockout
Lsm	Like-Sm
MDM	Mouse double minute homolog
MS/MS	tandem mass spectrometry
MTT	3-(4,5-dimethylthiazol-2-yl)-2,5-diphenyltetrazolium bromide
NB	Northern blot
NC	negative control
NLS	nuclear localization sequence
NMR	nuclear magnetic resonance
nt	nucleotide
NTC-NTR	NineTeen complex–NTC-related
NX	normalized expression
Oct	octamer-binding protein
PHAX	phosphorylated adaptor for RNA export
PIASy	protein inhibitor of activated STAT protein gamma
pICln	chloride ion current inducer protein
PIMT	protein L-isoaspartyl methyltransferase
PIPES	piperazine-N,N′-bis(2-ethanesulfonic acid)
PML	promyelocytic leukemia protein
PRPF	pre-mRNA processing factor
PSE	proximal sequence element
RT-qPCR	reverse transcription quantitative PCR

Ran	Ras-related nuclear protein
rRNA	ribosomal RNA
RT	room temperature
SART	squamous cell carcinoma antigen recognized by T-cells
scaRNA	small Cajal body-specific RNA
SEM	standard error of the mean
SF	splicing factor
SNAP	synaptosome associated protein
snoRNA	small nucleolar RNA
snRNA	small nuclear RNA
snRNP	small nuclear ribonucleoprotein
Snu	small nuclear ribonucleoprotein associated
ss	splice site
STAF	selenocysteine tRNA gene transcription-activating factor
TAF	TBP-associated factors
TBP	TATA-binding protein
TF	transcription factor
TUT	terminal uridylyltransferase
U2AF	U2 auxiliary factor
Unrip	unr-interacting protein
WB	Western blot
WT	wild type

1. Introduction

Biology of ribonucleoprotein complexes has been studied for years. RNA is capable of doing fascinating things in collaboration with proteins. Among those are protein synthesis (ribosomes), protection of genetic information during cell division (telomerase), splicing (spliceosome) and more.

Generally, eukaryotic genes are transcribed as precursors which are called pre-mRNA. They contain coding sequences (exons) and non-coding sequences (introns). Typically, in human, there are around two hundred base pair long exons interspersed with ten times longer introns. Splicing is a process of cutting out introns and joining exons so that a functional product – mRNA – is ready to proceed to the cytoplasm and serve as a template for protein synthesis. This is a multi-step process carried out and regulated by a huge number of participants. This thesis is mostly concerned with assembly, transport and quality control of small nuclear ribonucleoproteins which are constituents of a large spliceosomal complex.

Spliceosomal assembly happens along a convoluted pathway traversing a number of cellular compartments. Its RNA and protein compounds have to be produced and modified at an appropriate rate in the correct location. Coherently, it is not a surprise that quality control mechanisms are always in place. They strictly regulate competence of intermediates to be transported, join with other constituents or take part in splicing. Should those mechanisms fail, it may lead to pathological states like spinal muscular atrophy or retinitis pigmentosa.

One of the hubs involved in quality control is a Cajal body. It is a nuclear sub-compartment explicitly visible under the microscope in lots of metabolically active cells. In case small nuclear ribonucleoprotein structure is compromised, they accumulate in Cajal bodies in substantial quantities. One of the plausible mechanisms enabling accumulation is related to coilin. This protein is a Cajal body scaffold – a certain platform helping to bring together various molecules or even sequester the faulty ones. Is coilin a truly essential protein for small nuclear ribonucleoprotein quality control?

A gene knockout (KO) is a widely used technique to study gene function. This thesis inquires into possible differences in phenotype of normal cells in comparison to a coilin knockout cell line. By uncovering these differences, we would be able to better comprehend how important role coilin, and, by extension, Cajal bodies, play in spliceosomal assembly and function.

2. Literature review

2.1 Spliceosome

Spliceosome is a gigantic highly dynamic structure primarily involved into pre-mRNA splicing. It is of great importance because the vast majority of genes in higher eukaryotes contain introns that have to be spliced out to ensure functionality of the product. Spliceosomal complex is also notable due to the existence of alternative splicing, a mechanism behind striking diversity of different protein isoforms originating from a single gene. In this part of the literature review, we will sum up what is known about spliceosomal structure and function with principal focus on its RNA element.

2.1.1 Structure and Function

Various methods of structural analysis like X-ray crystallography, NMR studies and cryo-electron microscopy were employed to reveal what we know about the spliceosome nowadays. It is a multimegadalton complex composed of RNA with its core proteins and several associated non-snRNP proteins.

snRNA and associated proteins

The small nuclear ribonucleoprotein (snRNP) consists of a small nuclear RNA (snRNA) – U1, U2, U4/U6 or U5 – in complex with common Sm (or Like-Sm – LSm) proteins and other particle-specific core proteins. As visible from Fig. 2.1, snRNAs differ in their length and secondary structure. All but one snRNAs are transcribed by RNA polymerase II and acquire a trimethylguanosine cap, whereas U6 is transcribed by RNA polymerase III and has a gamma-monomethyl triphosphate guanosine cap (Reddy and Busch [1988], Singh and Reddy [1989]). The snRNAs are post-transcriptionally modified by pseudouridylases and 2′-O-methylases (extensively reviewed in Karijolich et al. [2010]). All spliceosomal snRNAs possess a U-rich sequence (Pu-A-U_{4-6}-G-Pu) in their 3′ region. It is known as Sm-site in U1, U2, U4 and U5 snRNA since a ring of Sm proteins is assembled there. A set of paralogous LSm proteins assemble on a similar U-rich LSm-site in case of U6 (Branlant et al. [1982]) .

There are at least ten proteins constituting each snRNP (Fig.2.1). Seven of them are "ever-present" Sm proteins – B, D1, D2, D3, E, F and G. As mentioned above, they form a characteristic ring on a short uridine-rich single stranded stretch of the snRNA, between two pronounced hairpins. The structural analysis by Pomeranz Krummel et al. [2009] and Grimm et al. [2013] showed that snRNA is threaded through the central hole of the ring. The Sm proteins are evolutionary well-conserved. Members of the Sm family contain a so-called "Sm fold" enabling binding to neighboring Sm proteins within a formed ring (Scofield and Lynch [2008]). The C-termini of B, D1 and D3 Sm proteins have an RG-rich region (e.g. RGRGRGMGRG position 110-119 of human Sm D3) known to be symmetrically methylated. This methylation is important for interaction with the survival motor neuron (SMN) complex and the Sm ring assembly on snRNAs (Meister et al. [2001b], Bradbury et al. [1975]).
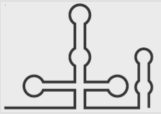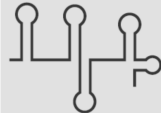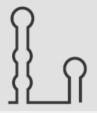
snRNP	snRNA		Sm and other core proteins associated with snRNA
U1	164 nt		B, D3, G, E, F, D2 and D1; U1-70K, U1A, U1C
U2	188 nt		B, D3, G, E, F, D2 and D1; U2A, U2B″, SF3B60, SF3A66, SF3A120, SF3B14B, SF3B14A, SF3B155, SF3B145, SF3B130, SF3B49 and SF3B10
U4/U6	144 nt and 107 nt		U4: B, D3, G, E, F, D2 and D1; U6: LSm2–8; PRPF3, PRPF31, PRPF4, 15.5K/NHPX, SART3, PPIH
U5	116 nt and 117 nt		B, D3, G, E, F, D2 and D1; PRPF8, PRPF6, DDX23, SNRNP200, EFTUD2, SNRNP40, CD2BP2 and TXNL4A

Figure 2.1: Composition of snRNPs [based on Matera and Wang [2014]]

Length and secondary structure of human snRNAs and protein composition of pertinent snRNPs are shown.

As mentioned earlier, instead of Sm complex U6 snRNA contains a ring of related but distinct Like-Sm proteins. They also contain a highly conserved Sm folds and their heptamers adopt a donut-like shape. The yeast LSm2–8 complex is known to associate with U6 snRNA in a different manner – by, so-called, "end recognition" or "capping": the 3′ end of U6 snRNA is anchored by LSm3 and the preceding three nucleotides are recognised by LSm2, LSm8 and LSm4 (Zhou et al. [2014]).

The U1 core proteins are not numerous making U1 snRNP the smallest among the spliceosomal snRNPs (Fig. 2.2b). Its structure has been solved in 2009 by Pomeranz Krummel et al. [2009]. One of the U1 snRNP proteins – U1C – contains a zinc-finger domain that stabilises the pre-mRNA/U1 snRNA interaction at the earliest steps of splicing (Kondo et al. [2015]). Other proteins known to associate with U1 snRNP in human function as alternative splicing factors facilitating recognition of weaker splice sites (Puig et al. [2007]).

The U2 snRNP elongated flexible structure has been well described for *S. cerevisiae* (Plaschka et al. [2017], Bai et al. [2018]). Apart from Sm-ring, there are a host of proteins (Fig. 2.1): the U2A-U2B hetero-dimer (Msl1-Lea1 in *S. cerevisiae*), SF3A (containing Prp9, Prp11, Prp21 in *S. cerevisiae*), and SF3B (containing Rds3, Hsh155, Cus1, Rse1, Hsh49 and Ysf3 in *S. cerevisiae*) subcomplexes. The SF3B proteins associate with 5′ end of U2 snRNA, whereas Sm ring and U2A-U2B associate with 3′ part, the SF3A subcomplex bridges the two – this creates a distinct bipartite arrangement of U2 snRNP rendering it limber and well-suited for the large scale movements during splicing (Fig. 2.2c).

The Y-shape tri-snRNP structure has been solved as well (Nguyen et al. [2015]). It is the largest pre-assembled complex made of U5 snRNA, U4/U6 snRNAs duplex and numerous proteins (Fig. 2.2a). In addition to the U5 and
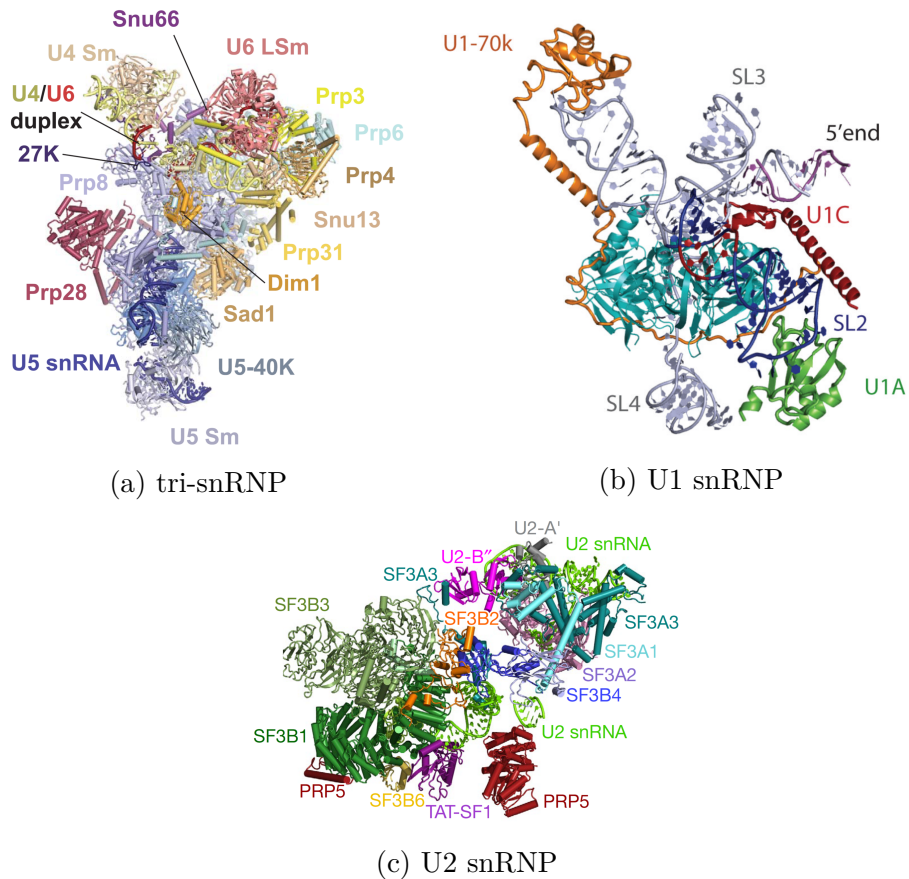
(a) tri-snRNP

(b) U1 snRNP

(c) U2 snRNP

Figure 2.2: U1, U2 and tri-snRNP structures, reproduced from [Pomeranz Krummel et al. [2009], Charenton et al. [2019], Zhang et al. [2020]]

U4/U6 specific proteins, the tri-snRNP also contains SNRNP27, SART1 and USP39 in its core. The key protein components of the tri-snRNP are PRPF8, PRPF6, SNRNP200 and EFTUD2. PRPF8 takes part in pre-mRNA positioning and closely associated with the catalytic RNA. PRPF8 accommodates the active site inside one of its domains after the spliceosomal activation – a maturase-like function (Galej et al. [2013]). PRPF6 is a helix–loop–helix motif rich protein (Makarov et al. [2000]). It is thought to form a bridge between U5 and U4/U6 snRNPs within the tri-snRNP (Liu et al. [2006]), and so, PRPF6 is vital for the correct assembly of this 1.5 MDa structure. SNRNP200 is a DExD/H box ATPase which catalyses disentanglement of the extensively base-paired U4/U6 snRNAs, crucial step of splicing (Raghunathan and Guthrie [1998]). EFTUD2 is a GTPase that controls SNRNP200 helicase activity (Small et al. [2006]).

There are a number of non-snRNP associated proteins which are vital for splicing. The most well-known examples are SF1 – a U2-associated protein recognising the branch site, and DHX16 in – one of the proteins driving transitions during the splice reaction (Shi [2017]).

Splicing

Splicing is a cotranscriptional process which means shared regulation and close cooperation with the transcriptional machinery (Das et al. [2006], Hicks et al. [2006]). It is necessary to mention that two different spliceosomal machineries exist in the vast majory of cells: the major (a.k.a. U2-dependent) and the less abundant minor (a.k.a. U12-dependent) spliceosome (Kreivi and Lamond [1996]). In this thesis, exclusively the first type will be described.

The main source of information for a proper splicing reaction to occur is the pre-mRNA itself. The sequences to be cut out – introns – are marked by short, conserved regions: 5′ splice site (5′ ss) and 3′ splice site (3′ ss). Additionally, inside the intron, upstream of the 3′ ss, another conserved region is located - branch site (BS). Other *cis*-acting elements are known including exonic and intronic splicing enhancers and silencers (Wang and Burge [2008]).

Regulation in *cis* alone is not sufficient to ensure the required degree of accuracy. It is when *de novo* assembly of the spliceosome comes in handy. By a stepwise process of its assembly, the spliceosome helps define exon-intron boundaries. The snRNAs play a central role as adaptors. They adjust pre-mRNA position in a favourable way for the reaction to occur. Moreover, the data acquired so far indicate that spliceosome is an RNP enzyme, and thus catalyses the splicing reaction (Matera et al. [2007]).
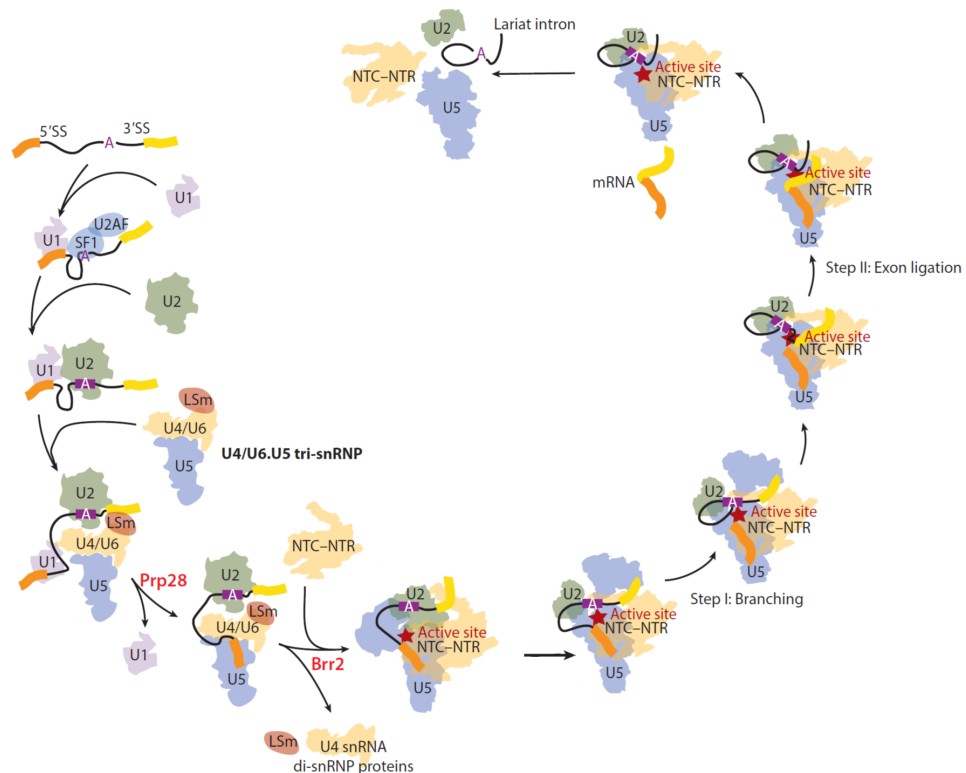

Figure 2.3: Splicing [reproduced from Wilkinson et al. [2020]]

The process starts with the U1 and U2 snRNPs marking the intron (the 5′ ss and the BS, respectively) based on sequence recognition, and recruiting the U4/U6.U5 tri-snRNP (Fig. 2.3). Next, with the aid of DDX23 DEAD-box

helicase, the $5'$ ss is transferred to base-pair with U6 snRNA instead of U1 snRNA causing release of the latter. After that, extensive base-pairing between U6 and U4 snRNAs is dissociated by SNRNP200 protein helicase activity. The separation causes a conformational change that brings together the crucial U6 and U2 snRNA moieties. Those fold into the spliceosome active centre harboring two metal ions necessary for coordination of trans-esterification reactions. The BS adenosine nucleophilic $2'$O attacks the phosphorus of $5'$ ss, resulting in a free $5'$ exon and the lariat–$3'$ exon intermediate. U5 snRNA is responsible for tethering the $5'$ exon to the spliceosome after the first reaction and alignment of both exons for the second one. Finally, the exons are ligated and the intron is removed by the second trans-esterification reaction between the $5'$ exon $3'$ OH group and the phosphorus atom of the $3'$ ss (Atkins [2011], Wilkinson et al. [2020]).

Despite this wealth of knowledge, our understanding of this mechanism is not complete. In particular, the transitions between spliceosomal conformations during splicing are not entirely without a gap, as well as the full extent of interactions between the spliceosome and RNA polymerase.

2.1.2 Biogenesis of spliceosomal snRNPs

Transcription and processing

All snRNAs, except of U6, are transcribed by RNA polymerase II. Their corresponding genes consist of a specific snRNA promoter, a coding region and a termination unit. The promoter stretches from distal sequence element (DSE) positioned at –220 to proximal sequence element (PSE) located at around –55 to the transcription start site. Another important feature of the transcription units of those snRNAs is a $3'$ box at 9–19 region downstream of the mature $3'$ end. The $3'$ box is crucial for the $3'$ end processing (Hernandez [2001], Hernandez [1985], Fischer et al. [2011]).

Opposed to the rest, U6 snRNA is transcribed by RNA polymerase III. In addition to DSE and PSE, its gene contains a TATA-box between PSE and the transcription start site. The $3'$ box is absent. Instead, there is a stretch of uridine residues at the snRNA $3'$ end (Hernandez [2001]).

Numerous trans-acting factors regulate transcription initiation of Sm-class snRNAs. In mammals, general transcription factors (TBP, TFIIB, TFIIA, TFIIF, TFIIE, TAF100 and probably TFIIH), as well as ubiquitous POU2F1, ZNF143 and pentameric SNAPC, bind to the promoter region allowing RNA polymerase II recruitment. The Integrator complex is also necessary for initiation, it binds to phosphorylated C-terminal domain (CTD) of the RNA polymerase. The processes of snRNA capping and $3'$ cleavage are thought to occur in tight association with transcription (Henry et al. [1998], Matera and Wang [2014]).

Apart from binding of PUO2F1 and ZNF143 to DSE and SNAPC to PSE, U6 gene transcription initiation requires TBP and the general RNA polymerase III specific factors (e.g. TFIIIB). U6 snRNA acquires a triphosphate guanosine cap. The gamma-monomethyl group on the cap is added post-transcriptionally (Reddy [1988]).

RNA synthesis continues beyond the mature 3'end of Sm-class snRNAs. The termination happens by means of an endonucleolytic cleavage at the 3' box. The Integrator complex, bound to the CTD as mentioned earlier, mediates the reac-

tion (Egloff et al. [2010], Matera and Wang [2014]). Following the 3' processing, the mature snRNA is exported to the cytoplasm.

It is probable that U6 snRNA termination happens via catalytic inactivation and backtracking of RNA polymerase III. The enzyme uses a poly-T stretch as termination signal (Nielsen et al. [2013]). Moreover, U6 snRNA is not exported to the cytoplasm for maturation but remains in the nucleus (Fischer et al. [2011], Hamm and Mattaj [1989]).

Export, cytoplasmic assembly and import

All snRNAs, except for U6, undergo cytoplasmic export, where first maturation steps take place (Fig. 2.4). The gene clusters of snRNA associate with a particular nuclear body – the Cajal body (CB) – and, interestingly, this association is mediated by the short nascent snRNA (Frey et al. [1999]). In fact, "pre-snRNA" is temporarily accumulated in the CB along with the associated proteins essential for export (Frey and Matera [2001], Suzuki et al. [2010]). The short transcripts are bound by the following mammalian proteins: CBP80, CBP20, PHAX and ARS2. NONO and SFPQ promote PHAX binding (Izaurralde et al. [1995], Ohno et al. [2000], Hallais et al. [2013], Izumi et al. [2014]). The bound proteins link the snRNA cap to an active exportin complex – CRM1/Ran/GTP, which promotes snRNA export via interaction with nuclear pore components. It appears that assembly of the to-be-exported complexes could be facilitated and surveyed in the CBs (Suzuki et al. [2010], Boulon et al. [2004]). Later, in the cytoplasm, Ran GTPase is able to hydrolyse GTP leading to the dissociation of the whole complex (Askjaer et al. [1999]). The snRNA has thus been exported and will now enter the cytoplasmic maturation phase.

Three major steps have to occur in order for the snRNP to be formed and imported back to the nucleus. Those are formation of the Sm core, hypermethylation of the cap and trimming of the 3' end.

A ring of seven Sm proteins, described in Section 2.1.1, assembles around the Sm site of snRNAs (Fig. 2.4). It is paramount for stabilisation of snRNP, protection against nucleases, as well as downstream processing and import (Matera and Wang [2014], Roithova et al. [2018], Roithova et al. [2020]). In mammals, the assembly is highly controlled by the survival motor neuron (SMN) protein, GEMINs 2-8 and unr-interacting protein (UNRIP) which together form the SMN complex (Meister et al. [2001a], Carissimi et al. [2005]). Three other proteins – methylosome protein 50, pICln and protein arginine N-methyltransferase 5 – participate in the assembly (Meister et al. [2001b], Meister and Fischer [2002]). They sequester Sm proteins, methylate Sm B, D1 and D3 and orchestrate formation of the Sm ring intermediate structures before association with the snRNA. It is known that GEMIN 5 in particular is responsible for the correct snRNA recruitment to the SMN complex (Yong et al. [2010]). At last, the SMN complex aids in the Sm ring closure around the snRNA rendering the core snRNP complete.

Next, snRNP is subjected to the cap hypermethylation by TGS1 – a human methyltransferase that converts a methylguanosine cap to a trimethylguanosine cap (Mouaikel et al. [2002]) – and the snRNA 3′ end is exonucleolytically processed by TOE1 (Hernandez and Weiner [1986], Lardelli and Lykke-Andersen [2020]).

Eventually, the Sm ring and trimethylguanosine cap serve as a signal that the snRNP is ready to be imported into the nucleus (Fig. 2.4). Snurportin 1, adaptor

for importin β, binds the cap (Huber et al. [1998]). The SMN complex could be imported alongside the core particle and appears to play a role in the snRNP binding to importin β (Narayanan et al. [2002]). It has been shown that depletion of importin β inhibits snRNP import into the nucleus (Palacios et al. [1997]).The snRNP enters the nucleus in an energy independent way (Huber et al. [2002], Wohlwend et al. [2007]).

Final maturation steps

While U1, U2, U4 and U5 snRNAs travel outside of the nucleus and back, U6 snRNA remains within its boundaries. Here it acquires a stretch of uridines on its $3'$ end added by human TUT1 (Lund and Dahlberg [1992], Trippe et al. [2006]). The uridines serve as a binding site for La proteins which protect the U6 snRNA $3'$ end before LSm ring assembles there (Achsel et al. [1999], Rinke and Steitz [1985]). The complex is relocated to the nucleolus, where it is subjected to $3'$ processing by specific enzymes (Gu et al. [1997]), pseudouridylation and $2'$-O-methylation by small nucleolar RNAs (Ganot et al. [1999]). Furthermore, the pre-formed LSm ring is also loaded onto U6 snRNA in the nucleolus, most probably in a single step (Licht et al. [2008]). After all the processing, U6 snRNA is transported to the CB in complex with SART3 to complete snRNP assembly including its annealing to U4 snRNA (Stanek et al. [2003]).

Loading of snRNP-specific proteins is aided by chaperons and takes place in the nucleus after the core particles are imported (Romac et al. [1994], Kambach and Mattaj [1994], Novotny et al. [2015]). These proteins contain NLS and it is thought that their import is independent of the core particles (Kambach and Mattaj [1992], Jantsch and Gall [1992]). The Cajal body is the place where Sm-class snRNAs accumulate right after the import (Sleeman and Lamond [1999]). Here, snRNAs get modified (pseudouridylation and 2'-O-methylation) with the aid of small Cajal-body specific RNA (scaRNA) (Jady et al. [2003]). As mentioned before, nucleotide modifications are crucial for snRNA stability, as they also increase the level of specificity when it is time for snRNP-specific proteins to bind (Yu et al. [1998]). The Cajal body assists in snRNP formation by providing a favourable chemical environment (Novotny et al. [2011]), especially by bringing snRNAs, associated proteins, chaperones, etc. into close proximity (see Section 2.2.2 for more detail). There is plenty of evidence suggesting that it is the site where specific proteins meet their RNA partners (Novotny et al. [2015],Bizarro et al. [2015]), and where assembly of U2 snRNP and tri-snRNP is finalised (Nesic et al. [2004], Schaffert et al. [2004], Stanek and Neugebauer [2004], Tanackovic and Kramer [2005]). In the CB, SART3 helps U6 and U4 snRNPs form the di-snRNP: it contains an RNA recognition motif that facilitates snRNA association. The following interactions with PRPF31, PRPF3 and PRPF4 promote the di-snRNP stabilisation (Nottrott et al. [2002]). To form a mature tri-snRNP, U5 snRNP incorporation is required. Until that time, immature di-snRNPs remain within the CBs (Schaffert et al. [2004], Stanek and Neugebauer [2004]). The most prominent protein component of U5 snRNP is PRPF8, through which the majority of protein-protein interactions occur. Therefore, association of U5 snRNA with PRPF8 is crucial for U5 snRNP integrity. Formation of the tri-snRNP is mediated by PRPF6, PRPF31 anf PRPF3 and additionally stabilised by snRNP27 (Novotny et al. [2015], Liu et al. [2006]).
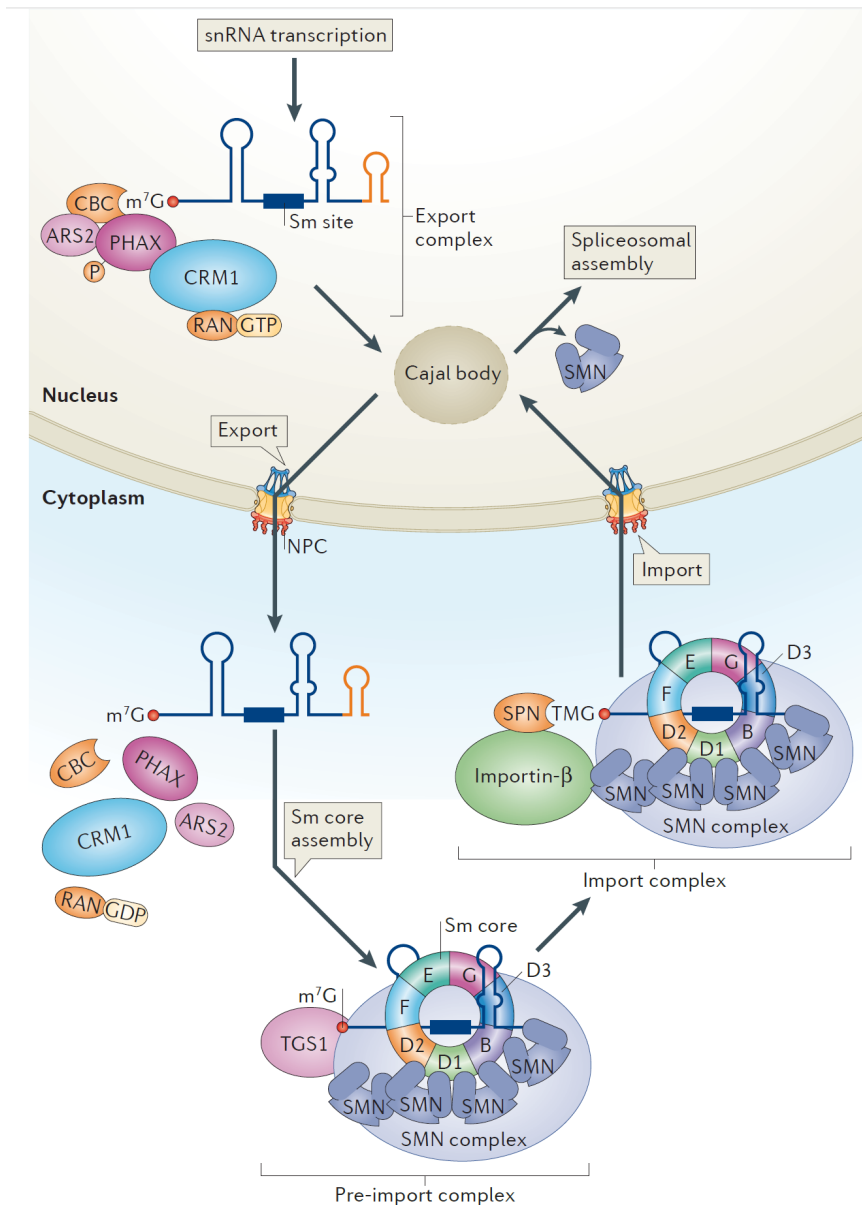
Figure 2.4: Biogenesis of Sm-class snRNP, reproduced from Matera and Wang [2014]

Export of pre-snRNAs, cytoplasmic maturation steps and re-import are shown. The export complex is assembled in the CB. Binding of several specific proteins, e.g. PHAX, is essential for export. After transport via the nuclear pore complex, the export complex dissociates. Cytoplasmic maturation steps governed by the SMN complex take place. Loading of the symmetrically dimethylated Sm proteins onto the Sm site of snRNA finalises the core formation. Hypermethylation and 3′-end trimming follow. Then, the import complex is assembled by recruitment of importin β. After nuclear import, the snRNPs localise in the CBs. Here, snRNAs are modified and joint with other snRNP-specific proteins to produce mature snRNP particles.

The snRNP biogenesis reaches completion when higher order spliceosomal structures, those competent to engage with the splicing machinery, are assembled. After that, U1, U2 snRNPs and U4/U6.U5 tri-snRNP localise to nuclear speckles functioning as a storage compartment for splicing factors (Sleeman and Lamond [1999]).

2.2 Coilin

Coilin (UniProtKB: P38432) is a 63 kDa protein first visualised by human autoimmune antibodies. Under the microscope, it generally exhibits a sublime staining pattern of a number of explicit foci in the nucleus in addition to a diffuse nucleoplasmic pool (Andrade et al. [1991], Raska et al. [1991]). Coilin is a ubiquitous protein enriched in testis, in early and late spermatids (Thul et al. [2017], Human Protein Atlas available from http://www.proteinatlas.org).
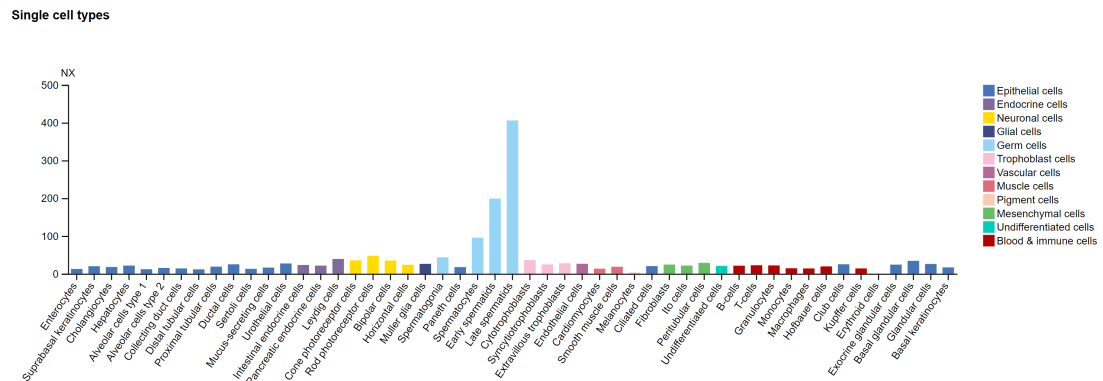

Figure 2.5: Human transcriptomics data from single cell types for coilin, reproduced from [Human Protein Atlas]

In *Homo sapiens*, it is encoded by a 7-exon gene on 17q22 (NCBI ID: 8161). Two transcripts are predicted: one full-lenght, confirmed experimentally to result in a 576 amino acid polypeptide; and another short putative splice variant, possibly resulting in a 37 amino acid polypeptide aligning with 81-109 region of the full-lenght protein. This gene has pseudogenes on chromosome 4 and chromosome 14. Coilin is widely accepted as a Cajal body marker protein, however, its structure and function are still poorly understood.

2.2.1 Structure

The most conserved regions of coilin are its N- and C-termini. The N-terminus is crucial for coilin's ability to self-interact. It appears to be a common theme for other nuclear body specific proteins – they are also able to self-oligomerise (e.g. PML, SMN and SAM68) – underlining a common feature assisting a highly organised eukaryotic nucleus in existence (Lorson et al. [1998], Chen et al. [1999], Ishov et al. [1999]). In fact, the coilin first 92 amino acid residues are necessary and sufficient to localise a protein to Cajal bodies (Hebert and Matera [2000]). The low complexity middle part of the protein does not seem to be conserved (Machyna et al. [2015]). There are two nuclear localisation signals. Between

them, in the position 160-168, a cryptic nucleolar localisation signal, MDM2-like basic sequence, has been reported (Hebert and Matera [2000]). Based on this finding, one could speculate that coilin possesses an ability to fold alternatively and interact with components of the nucleolus.

Coilin is a phosphoprotein phosphorylation of which was thought to be cell-cycle dependent and to only occur on serine residues (Carmo-Fonseca et al. [1993]). There are several serine patches at 242–259 and at 312–325 which could be potentially phosphorylated, as well as a consensus phosphorylation site at S184 (Hebert and Matera [2000], Sanz-Garcia et al. [2011]). Recent tandem MS/MS analysis indicated phosphorylation of several amino acids in the middle region (T122, S271, S272, T303, S489) and presence of six C-terminal phosphoresidues important for proper localisation (S566, S568, T570, S571, S572, T573) (Hearst et al. [2009]). An arginine and glycin rich region, the so-called RG box, found at 392-420 is required for interaction with the SMN complex and appears to be specific for vertebrates (Hebert et al. [2001]).

Coilin C-terminus, being well-conserved, adopts a Tudor domain-like structure which bears numerous similarities to the domains like "Kyprides, Ouzounis, Woese", "conserved domain within Cul7, PARC, and HERC2 proteins" and "SRC Homology 3" (Shanbhag et al. [2010]). This implicates coilin's potential to bind methylated amino acids like symmetrically dimethylated arginines present in Sm proteins. However, a combination of bioinformatics, deletion analysis and NMR spectroscopy performed by (Shanbhag et al. [2010]) did not reveal any obvious amino acid patterns in favour of such an implication.

2.2.2 Function

Viewed primarily as a Cajal body marker and scaffold protein, coilin function is tightly related to this nuclear sub-compartment. However, Lam et al. [2002] report that only 30% of coilin resides there, the rest is nucleoplasmic. Cajal bodies disappear during mitosis and reform in the early interphase, with the highest number of them being present at mid to late G1. Interestingly, coilin level remains constant throughout the cell cycle (Andrade et al. [1993]), however, its phosphorylation status does not, pointing out the mechanism by which integrity of the Cajal bodies is regulated (Carmo-Fonseca et al. [1993], Hebert and Matera [2000]). Gems are another nuclear structure rich in coilin since they often co-localise with Cajal bodies and contain similar proteins, like SMN complex. It was suggested that methylation of coilin RG box determines whether the SMN complex is transported to gems or to Cajal bodies (Hebert et al. [2002]).

The Cajal body, first described by Ramon-y-Cajal in neuronal cells, is a curious nuclear domain ranging from 0.15 to over 1.5 μm in diameter. Coilin is required for formation of the Cajal bodies in *Homo sapiens* (Carmo-Fonseca et al. [1993]), in *Mus musculus* (Tucker et al. [2001]), *Drosophila melanogaster* (Liu et al. [2009]), and in *Danio rerio* (Strzelecka et al. [2010]). The data provided by Kaiser et al. [2008] showed that the Cajal body can be formed *de novo* in presence of its constituents (coilin, SMN complex, spliceosomal snRNPs and scaRNPs), and assembles as a self-organising structure. It was suggested that the Cajal body is an snRNP maturation site (Matera and Shpargel [2006]). Therefore, it is rational to assume that coilin itself plays a notable role in snRNP metabolism.

First of all, coilin brings together various components like: i. relevant threads of chromatin – genes for histones and snRNAs (Machyna et al. [2014]), U4, U11, and U12 snRNA loci (Jacobs et al. [1999]), as well as U2 and U1 snRNA loci (Smith et al. [1995]); ii. RNA molecules – snRNA, scaRNA (Enwerem et al. [2014]), snoRNA (Boulon et al. [2004], Machyna et al. [2014]); iii. protein factors – Sm proteins (Xu et al. [2005]), SART3 (Novotny et al. [2015]), a subunit of Integrator complex (Takata et al. [2012]), nucleolar and coiled-body phospho-protein 1 (Nopp140) (Isaac et al. [1998]), ankyrin repeat and sterile alpha motif domain-containing protein 1B (AIDA1c)(Xu and Hebert [2005]) etc. The particular sites of interaction are in Fig. 2.6. By this, coilin sets up a favourable environment for the appropriate biochemical processes to take place, as well as providing a plausible mechanism how to sequester faulty participants from the snRNP biogenesis pathway.
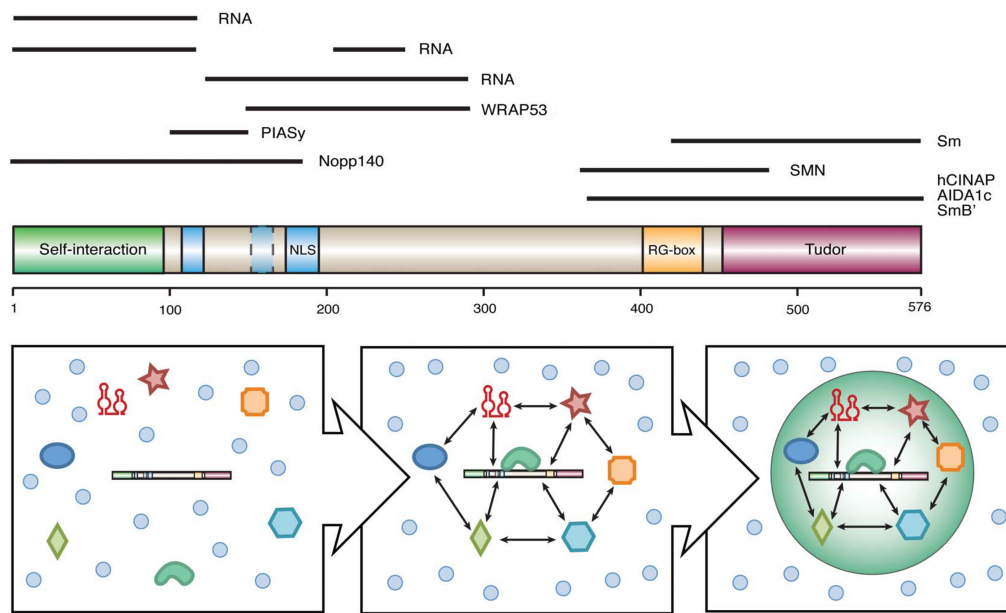

Figure 2.6: Coilin schematic structure, interaction partners and formation of the Cajal body [reproduced from Machyna et al. [2015]]

Secondly, during their biogenesis, as was described in 2.1.2, snRNA and proteins participating in the snRNP assembly frequently enter and leave the Cajal body. Probably, there is a CB-associated snRNA surveillance step before the snRNA exit from the nucleus into the cytoplasm, since export-related proteins are found within the CB. Next, the snRNP components pass through it after they return or are *de novo* imported into the nucleus. Their transient localisation is a clear sign of the CB-mediated facilitation and RNP remodeling taking place. Presence of binding sites for major snRNA associated proteins like Sm, SMN, SART3 etc., in coilin only reinforces the point. Moreover, depletion of PHAX, knockdown of snRNP-specific proteins or impediment of the tri-snRNP formation, in other words, anything that might lead to increased concentration of defected snRNPs, triggers snRNA accumulation in and even *de novo* formation of Cajal bodies in the cell type normally lacking those structures (Novotny et al. [2015], Schaffert et al. [2004], Suzuki et al. [2010]. In concordance with that, transfor-

mation process, associated with high levels of transcription and thus splicing, also induces Cajal body formation (Spector et al. [1992]). On the other hand, as Lemm et al. [2006] showed, Cajal bodies disintegrate upon SMN or PHAX RNAi-mediated depletion. In those cases, coilin is dispersed in the nucleoplasm. It has been recently shown that snRNPs accumulate in the CB in the Sm ring-dependent manner (Roithova et al. [2018]). Therefore, there should be a factors that is able to tether immature snRNPs via interaction with the Sm-ring. Coilin is known to interact with individual Sm proteins. This suggests that coilin in particular might be the factor that discriminate between mature and immature snRNPs. The fate of snRNPs accumulated in the CB is unknown: they could be stabilised for maturation completion or get degraded.

On top of all mentioned above, *in vivo* studies in mice and fish showed that without coilin embryogenesis, fertility and even viability could be compromised (Tucker et al. [2001], Strzelecka et al. [2010]). This strong effect on reproductive function, especially in mice, points at the CB role in highly active cells like embryonic, transformed or neuronal cells.

On the other hand, a number of differentiated cell types do not contain any visible Cajal bodies indicating that their presence is not of critical importance (Whittom et al. [2008]). Moreover, experiments in flies (Liu et al. [2009]) did not show any detectable fertility decrease in coilin-null mutants. It means that, under certain conditions, snRNP particles can assemble and recycle properly without help of coilin. From the data analysed, it appears that aggregation of all the necessary components inside the CB reflects the intensity of snRNP metabolism rather than represent a feature fundamental for survival.

This ambiguity and incomplete understanding of coilin molecular function prompted us to further investigate the relationship between snRNP biogenesis and the CB major scaffold protein coilin.

3. Aims of the thesis

We intended to test a hypothesis that coilin is a part of the control machinery that monitors snRNP biogenesis. The primary goal of this thesis was to evaluate the response of coilin-deficient cells under conditions of spliceosomal assembly malfunction in order to understand the role Cajal bodies play in the fate of incomplete snRNP particles.

In all three experimental parts, these conditions were achieved by performing an siRNA-mediated knockdown of the snRNP component proteins resulting in increased concentration of stalled tri-snRNP precursors.

The first part pursued the goal through visualisation of apparent differences in coilin knockout cell phenotype. The second part was dedicated to assessment of the coilin-deficient cells proliferation rate through analysis of cell viability. Lastly, we aimed to estimate the change in snRNA steady state levels by means of RNA quantification techniques.

4. Materials and methods

4.1 Materials

4.1.1 siRNA, hybridisation probes, primers and antibodies

siRNA	Sequence (5′ to 3′)	Manufacturer
NC5 (Silencer Negative Control 5 siRNA)		Ambion
PRPF6-siRNA	AGGUUCCGAGCUACUUGUAGCtt	Ambion
PRPF31-siRNA	AAGCCAAAGCTTCAGAAGTtt	Ambion
PRPF8-siRNA	CCUGUAUGCCUGACCGUUUtt	Ambion

Table 4.1: List of siRNAs

Target RNA	Sequence (5′ to 3′)	Purpose
U4 snRNA	CCAGTGCCGACTATATTGCAAGTCGTCACG	NB
U4 snRNA	TCACGGCGGGGTATTGGGAAAAGTTTTCAATTAG-CAATATCGCGCCT	FISH
U5 snRNA	TTGGGTTAAGACTCAGAGTTGTTCCTCTCC	NB
U5 snRNA	CTCTCCACGGAAATCTTTAGTAAAAGGCGAAAGA-TTTATACGATTTGAAGAG	FISH
U6 snRNA	CACGAATTTGCGTGTCATCCTTGCGCAGGGGCCAT	NB
U2 snRNA	GAACAGATACTACACTTGATCTTAGCCAAAAGG-CCGAGA	FISH
5S rRNA	TCTCCCATCCAAGTACTAACCAGGCCCGACC	NB

Table 4.2: List of hybridisation probes

Primer	Sequence (5′ to 3′)	Purpose
Random	NNNNNN	Reverse transcription
U4 snRNA$_F$	TGGCAGTATCGTAGCCAATG	qPCR
U4 snRNA$_R$	CTGTCAAAAATTGCCAGTGC	qPCR
U5 snRNA$_F$	CTCTGGTTTCTCTTCAGATC	qPCR
U5 snRNA$_R$	TGTTCCTCTCCACGGAAATC	qPCR
U6 snRNA$_F$	CGCTTCGGCAGCACATATAC	qPCR
U6 snRNA$_R$	AAAATATGGAACGCTTCACGA	qPCR
7SK RNA$_F$	GGAGGATCCGAGGGCGATCTGGCTGCGAC	qPCR
7SK RNA$_R$	GCGGAATTCCGCAGATGGAGCGGTGAGGC	qPCR

Table 4.3: List of primers

Antibody	Origin	Manufacturer	Purpose
anti-PRPF31	rabbit	Abcam	WB
anti-PRPF6	mouse	Santa Cruz Biotechnology	WB
anti-PRPF8	mouse	Santa Cruz Biotechnology	WB
anti-GAPDH	mouse	Abcam	WB
anti-alfa tubulin	mouse	Facility of IMG ASCR	WB

Table 4.4: List of antibodies

4.1.2 Solutions

3M NaCl
300mM sodium citrate, pH 7.0

Table 4.5: 20x SSC buffer

4x SSC
2% (wt/vol) BSA
20% (wt/vol) dextran sulfate solution

Table 4.6: RNA FISH hybridisation mix

25mM Tris-HCl
192mM glycine
0.1% (wt/vol) SDS

Table 4.7: SDS running buffer

40% acrylamide/N,N'-methylene-bisacrylamide 37.5:1	1.25 ml
1.5M Tris-HCl pH 8.8	1.25 ml
10% SDS	25 μl
dH2O	2.42 ml
10% APS	50 μl
TEMED	2 μl

Table 4.8: Separating gel, 10% (5 ml vol.)

40% acrylamide/N,N'-methylene-bisacrylamide 37.5:1	310 μl
1M Tris-HCl pH 6.8	310 μl
10% SDS	13 μl
dH2O	1.83 ml
10% APS	25 μl
TEMED	3 μl

Table 4.9: Stacking gel (2.5 ml vol.)

25mM Tris-HCl
192mM glycine
20% (vol/vol) methanol

Table 4.10: WB transfer buffer

5x TBE	2 ml
40% acrylamide/N,N'-methylene-bis-acrylamide 19:1	3.35 ml
10% APS	100 μl
TEMED	5 μl

Table 4.11: RNA separating gel (10 ml vol.)

0.5M Tris base
0.5M boric acid
0.01M EDTA (pH 8.0)

Table 4.12: 5X TBE stock solution

0.25M sodium phosphate buffer pH 7.2
1mM EDTA
1% (wt/vol) BSA
7% (wt/vol) SDS

Table 4.13: Church buffer

40% (vol/vol) dimethylformamide
2% (vol/vol) glacial acetic acid
16% (wt/vol) SDS

Table 4.14: DMF solubilisation solution

4.2   Methods

4.2.1   Cell culture

All the experiments were done using HeLa cells which grew in Dulbecco's Modified Eagle's Medium with high glucose (Sigma-Aldrich) supplemented with 10% fetal bovine serum and antibiotics (penicillin and streptomycin). Cells were cultured in 5% CO_2 atmosphere at 37°C.

20% (vol/vol) glycerol
2% (vol/vol) 2-mercaptoethanol
4% (wt/vol) SDS
250 mM Tris-HCl pH 6.8
0.02% (wt/vol) bromophenol blue

Table 4.15: 2x sample buffer

4.2.2 Transfection of siRNA

HeLa cells were grown in culture till 50% confluent. All siRNAs were transfected using Oligofectamine (Invitrogen) in line with the manufacturer's protocol - the transfection reagent and the $20\mu M$ siRNA were incubated in Opti-MEM medium at room temperature for 5 min, mixed, incubated for further 20 min and added to the cell medium. The cells remained in culture for 48 h before proceeding to downstream experiments.

For MTT assay knockdown effect assessment, the cells were transfected on the day of seeding. The exposition time is specified in Chapter 5.

Culture vessel	siRNA and dilution vol.	Oligofectamine and dilution vol.
6-well plate	5 μl in 70 μl	5 μl in 20 μl
24-well plate	1.25 μl in 17.5 μl	1.25 μl in 17.5 μl

Table 4.16: Transfection mix

4.2.3 MTT assay

HeLa cells were seeded in 24-well plates at different densities for: i. calibration - two fold serial dilution from 20 x 10^4 to 2.5 x 10^4 per well; ii. growth assessment - 1.25 x 10^4 per well and iii. knockdown effect assessment - 5 x 10^4 per well.

MTT solution (5 mg/ml in PBS – stock solution) was added to the final concentration of 0.22 mg/ml: i. calibration - two hours after seeding; ii. growth assessment - after 24 h, 48 h and 72 h of standard cultivation; iii. knockdown effect assessment - 24 h, 48 h and 72 h after transfection.

The cells were incubated for 3 h in 5% CO_2 atmosphere at 37°C. MTT formazan crystals were then resolved by adding 0.5 ml of DMF solubilisation solution (Table 4.14). The resulting mixture was pipetted up and down for better solubilisation and stayed on a shaker as long as crystals remain visible. Absorbance was measured at a wavelength of 540 nm, and background substracted at 630 nm, using a microplate reader (EnVision Multilabel Reader, PerkinElmer).

4.2.4 Preparation of cell lysate

HeLa cells grew in a 6-well plate. They were washed two times with PBS. To each well, 200 μl of 2x sample buffer (Table 4.15) were added and the cells scraped off the surface. The resulting suspension was collected and subjected to sonication. The samples were incubated at 95°C for 5 min and then stored at

-20°C. The lysate was used for the knockdown efficiency assessment via Western blotting.

4.2.5   Isolation of RNA

HeLa cells grew in a 6-well plate. They were washed once with PBS. Sufficient volume of TRIzol™ reagent was added to the well in accordance with the manufacturer's instructions. The cells were incubated for 5 min at RT and transferred to a tube. Then, chloroform was added at ratio 0.2 ml per 1 ml of TRIzol™ and the cells were incubated for 3 min at RT. Centrifugation (15 min, 14,000×g, 4°C) followed. Colorless upper aqueous phase containing RNA was precipitated using equal volume of isopropanol and glycogen carrier for 1 h at -25°C. Centrifugation (15 min, 14,000×g, 4°C) followed. The resulting pellet was washed with 70% ethanol. After that, it was resuspended in RNase free water and either solubilised at 60°C for 10 min and used in Northern blot analysis or was subjected to DNase treatment for qRT-PCR analysis.

The treatment was carried out by TURBO™ DNase (Ambion) in the supplied digestion buffer at 37°C for 45 min. The resulting mixture was re-purified by precipitating in 62.5% ethanol, 0.375 M sodium acetate solution at -80°C for 1 h. Centrifugation (20 min, 14,000×g, 4°C) followed. The resulting pellet was washed two times with 70% ethanol and resuspended in RNase free water.

4.2.6   RT-qPCR

Reverse transcription was done on the same day as RNA isolation to prevent RNA degradation from affecting the result of the experiments. For each reaction, 5 μg of total RNA were used.

total RNA	5 μg
random hexamers (250 ng/μl)	1 μl
dH$_2$0	up to 20 μl vol.

Table 4.17: Pre-incubation reaction mix

The reaction mix was incubated at 65°C for 5 min to denature the target RNA, and then rapidly chilled to 4°C. After that, the reagents from Table 4.18 were added. The resulting mixture was, first, incubated at 25 °C for 5 min, next, at 50°C for 90 min, and finally, at 70°C for 15 min to inactivate the enzyme.

5x First Strand buffer (Invitrogen)	4 μl
10mM dNTPs	1 μl
0.1M DTT (Invitrogen)	1 μl
SuperScript III Reverse Transcriptase (Invitrogen)	0.5 μl

Table 4.18: Reagents added after RNA denaturation incubation

Acquired complementary DNA (cDNA) was diluted 1:19 for U1, U4, U5 and U6 snRNAs qPCR reactions and 1:199 for 7SK RNA. The cDNA and qPCR Master Mix were separately transferred to the designated wells. The samples were loaded on the plate in duplicates.

cDNA	2 μl
SYBR Green I Master (Roche)	2.5 μl
10 μM primer F	0.25 μl
10 μM primer R	0.25 μl

Table 4.19: qPCR Master Mix

Initial denaturation	95 °C	7 min	1 cycle
Quantification:			
Denaturation	95 °C	20 s	
Annealing	61 °C	20 s	40 cycles
Elongation	72 °C	35 s	
Melting curves analysis	95 °C	15 s	
	55 °C	1 min 1 s	1 cycle
	37 °C	1 min 1 s	

Table 4.20: qPCR program

The arithmetic mean of Ct values for different snRNAs was calculated and normalised to 7SK RNA values according to the following equation:

$$N = 2^{Ct_{snRNA} - Ct_{7SK}}$$

4.2.7 Denaturing RNA PAGE

RNA was processed on the day of isolation to prevent RNA degradation from affecting results of the experiment. Its quality and concentration was determined spectrophotometrically. Bio-Rad Mini-PROTEAN system was utilised. Hand-cast 10% TBE PAGE gels used in all the experiments were prepared according to the Table 4.11. Shortly before electrophoresis, approximately 5 ng of RNA were mixed with 2x Gel Loading Buffer II (Ambion), containing 95% formamide, 18 mM EDTA, 0.025% SDS, xylene cyanol, and bromophenol blue, and incubated at 65°C for 6 min. PageRuler Plus pre-stained protein ladder (Thermo Scientific) was loaded onto gels for size reference in downstream applications. The RNA was separated at a voltage gradient of 5 V/cm in 0.5x TBE buffer for 60 min (Table 4.12).

4.2.8 GelStar staining

The gel was stained with GelStar™ nucleic acid gel stain (Lonza Rockland), 5 μl of the supplied stock solution in 10 ml of 0.5x TBE for 5 min at RT. Subsequently, it was visualised using Molecular Imager Gel Doc XR (Bio-Rad).

4.2.9 Fluorescent Northern blotting

Before blotting, a nylon membrane (Zeta-Probe, Bio-Rad), filter papers and sponges were soaked in 0.5x TBE. A blotting sandwich was constructed according to the Bio-Rad wet blotting guide. Transfer was performed at a constant current of 360 mA for 60 min. After transfer, the membrane was crosslinked at

Autocrosslink setting on Stratalinker (Stratagene), dried up and stored at RT before hybridisation.

Hybridisation was carried out in the mini-oven (Hybaid). First, the membrane was pre-hybridised in Church buffer (Table 4.13) at 55°C for 2 h. Then, it was hybridised with 100 nM probe in Church buffer overnight at 55°C. After that, the membrane was washed twice, 10 min each, with Wash buffer-1 (2x SSC, 0.1% SDS, 55°C) and twice, 10 min each, with Wash buffer-2 (0.2x SSC, 0.1% SDS, RT).

The image was developed using Amersham Typhoon Biomolecular Imager and analysed with Image Lab software (Bio-Rad).

4.2.10 SDS PAGE

Bio-Rad Mini-PROTEAN system was utilised. Handcast 10% SDS PAGE gels used in all the experiments were prepared according to the manufacturer instructions, see Table 4.8 and Table 4.9. PageRuler Plus pre-stained protein ladder (Thermo Scientific) was loaded onto gels for monitoring protein migration and as a size standard for downstream applications. Proteins were separated at 120 V for approximately 60 min.

4.2.11 Western blotting

Before blotting, the gel, a nitrocellulose membrane (0.45 μm, Amersham Protran, GE Healthcare), filter papers and sponges were soaked in the transfer buffer (Table 4.10). Transfer was performed using Bio-Rad wet blotting system at a constant current of 360 mA for 80 min. A blotting sandwich was constructed according to the manufacturer instructions.

Following transfer, the resulting membrane was washed in PBST (PBS with 0.05% Tween) and blocked in 5% low fat milk/PBST for 1 h. After that, the membrane was incubated at 4°C in a solution containing the primary antibody diluted to required concentration in 1% low fat milk/PBST for 90 min. It was washed three times with PBST. Finally, the membrane was stained with an appropriate secondary antibody diluted in 1% low fat milk/PBST for 1 h. Three washes in PBST followed.

For all the experiments, either anti-mouse or anti-rabbit AffiniPure goat secondary antibody conjugated with HRP (Jackson ImmunoResearch) was used. The membrane was incubated with SuperSignal West chemiluminescent substrate (Thermo Scientific) and developed using Alliance Q9-ATOM Light (Thistle Scientific).

4.2.12 Immunofluorescent staining and FISH

Cells were grown in a 24-well plate on glass coverslips. The cells were washed three times with 0.5 ml of PBS, and then fixed with 4% PFA/PIPES for 10 min. They were washed again, three times with PBS buffer, and subsequently permeabilised with 0.5% Triton X-100/PBS for 5 min. After three more washes with PBS, the cells were quenched in 0.1 M glycine/0.2 M Tris-HCl pH 7.4 for 5 min. They were washed once more. Prior to the the hybridisation step, coverslips

were placed in 2x SSC/50% formamide for 10 min. Hybridisation in a humidified chamber at 37°C on drops of 7.5 μl of formamide + 7.5 μl of FISH master mix (Table 4.6) + 0.5 μl of fluorescent probe for 1 h followed.

After the hybridisation step, the cells were washed with 2x SSC/50% formamide at 37°C for 20 min, and then with 2x SSC alone in the same conditions. Finally, the cells were incubated in 1x SSC at room temperature for 20 min. The coverslips were left to dry up for 30 min and then mounted to microscope slides using DAPI Fluoromount-G medium (SouthernBiotech).

The cells were visualised using DeltaVision microscopic system (Applied Precision) mounted onto Olympus IX70 microscope. The microscope oil immersion objective (60x/1.4 NA) was used to acquire twenty Z-stacks with 200 nm spacing. Image restoration included deconvolution done via SoftWorx deconvolution system (Applied Precision). Image analysis and processing were done in the ImageJ program (Schindelin et al. [2012]).

5. Results

The coilin knockout (KO) cell line was generated – COIL alleles were deleted using CRISPR/Cas9 technology – and kindly provided for the following experiments by Davide Alessandro Basello (manuscript in preparation). The cells did not express coilin and lacked visible Cajal bodies.

5.1 Coilin knockout cells are unable to sequester misfolded snRNP particles

First of all, it was vital to make sure we knew what we were working with. The method of choice was visualisation enabling us to observe the cell phenotype directly. Our experiment has been inspired by the publication of Novotny et al. [2015] showing that inhibition of the tri-snRNP assembly pathway induces CB formation in the cells normally lacking them.

We reasoned that fluorescence *in situ* hybridisation (FISH) detection of U4, U5 and U2 snRNAs could show us how wild type (WT) and coilin knockout cell lines react under the conditions of increased concentration of stalled snRNPs and greater need of quality control. Correspondingly, PRPF6 was downregulated in order to mimic such conditions (for representative efficiency of the knockdown (KD) see Fig. 5.9a). Localisation of U4, U5 and U2 snRNAs was analysed.
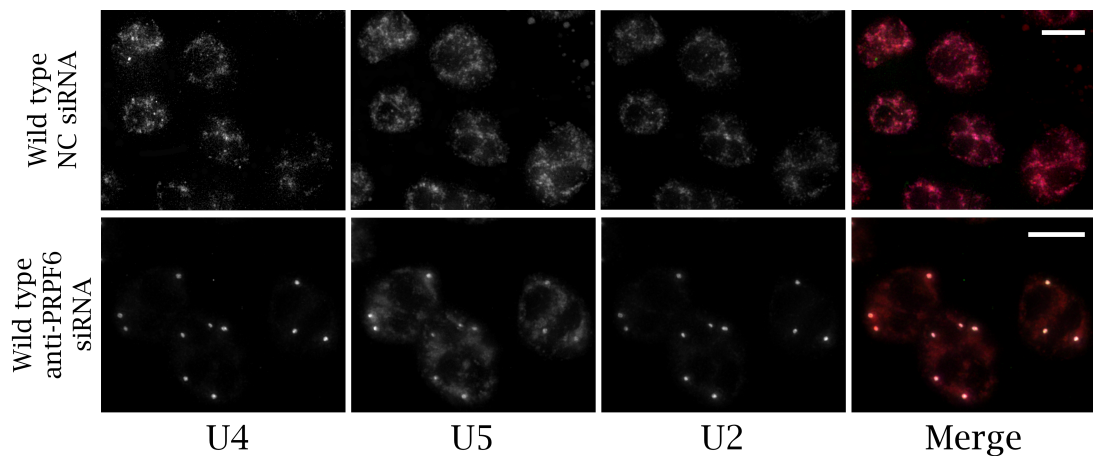
Figure 5.1: Effect of PRPF6 knockdown on HeLa wild type cell line

Hela wild type cells were treated with negative control siRNA (NC, top panel) and siRNA against PRPF6 (anti-PRPF6, bottom panel). The snRNA localisation monitored by FISH. Knockdown of PRPF6 led to extensive U4, U5 and U2 snRNA accumulation in nuclear bodies visible as clearly distinct numerous foci. The merge images of all three channels are shown: U4 - 488 (green), U5 - Cy3 (red) and U2 - Cy5 (magenta).The scale bar represents 10 μm.

Cells treated with negative control (NC) siRNA were characterised by proper localisation and normal distribution of snRNA in the nucleus. There was a clear

response in HeLa WT cell line upon addition of anti-PRPF6 siRNA (Fig. 5.1). Vast majority of U4, U5 and U2 snRNA accumulated in nuclear bodies, which were previously shown to be Cajal bodies (Novotny et al. [2015]), and almost none except for U5 snRNA was found in the nucleoplasm. U5 snRNA is not fully localised to the bodies and remains in the nucleoplasm to a visibly greater extent than U4 and U2.
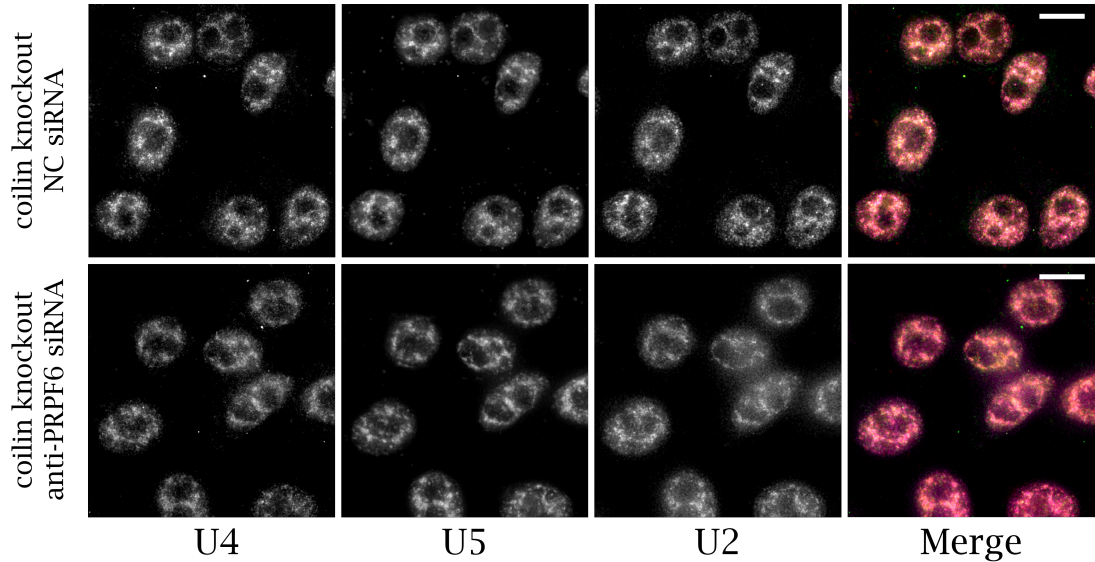

Figure 5.2: Effect of PRPF6 knockdown on HeLa coilin knockout cell line

Hela coilin KO cells were treated with negative control siRNA (NC, top panel) and siRNA against PRPF6 (anti-PRPF6, bottom panel). The snRNA localisation monitored by FISH. In either case, we did not observe any sequestration of snRNA. The merge images of all three channels are shown: U4 - 488 (green), U5 - Cy3 (red) and U2 - Cy5 (magenta).The scale bar represents 10 μm.

It was not the case for the coilin knockout cell line (Fig. 5.2). Cells treated with NC siRNA were quite distinct from the WT. Diffuse nucleoplasmic staining of snRNA could be observed as an evident result of coilin knockout. It also looks as if NC coilin KO nuclei were slightly smaller in diameter than in NC WT. Even though the correct assembly of snRNPs had been disrupted by knockdown of PRPF6, almost all the U4, U5 and U2 snRNAs were dispersed in the nucleoplasm. The cells were unable to sequester the stalled snRNPs to any visible extent. In all respects, the cells looked similar to control.

A clear dissimilarity of the cell response to the malfunction in snRNP biogenesis prompted us to further investigate a degree of the cell lines functional divergence.

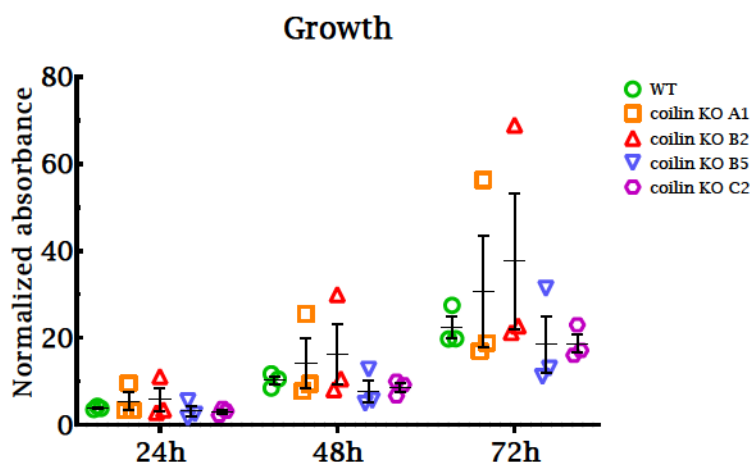## 5.2 Coilin knockout cell proliferation was not significantly different from the wild type

Figure 5.3: Growth of HeLa wild type, coilin knockout A1, B2, B5 and C2 cell lines

Cell viability was measured by MTT assay. The growth is displayed as a change in absorbance at 490 nm after 24, 48 and 72 hours in culture. The normalised value was calculated via dividing the resulting absorbance by the absorbance immediately after seeding. The data are represented as individual measurements with mean and SEM bars.

We started with evaluation of HeLa wild type and HeLa coilin knockout viability. Our presumption was that since the coilin KO cells were not able to sequester misfolded snRNPs in the CB, they might have difficulty coping with their increased concentration and proliferate slower.

First of all, we compared growth of HeLa WT cell line to four clonal HeLa coilin KO cell lines. Such redundancy in the number of clonal coilin KO cell lines was implemented due to a well-known consequence of excessive subculturing that increases the risk of phenotypic alteration, especially in CRISPR/Cas9 generated cultures. MTT assay, one of the most commonly used colorimetric methods to estimate the number of viable cells, was chosen (Riss et al. [2004]). This procedure is based on tetrazolium compound reduction by NADH utilizing cell enzymes. In addition to the mere number of cells, the amount of signal detected depends on parameters such as MTT concentration, incubation period duration and cellular metabolic activity. The protocol was carefully optimised to achieve satisfactory assay conditions (see Section 4.2.3).
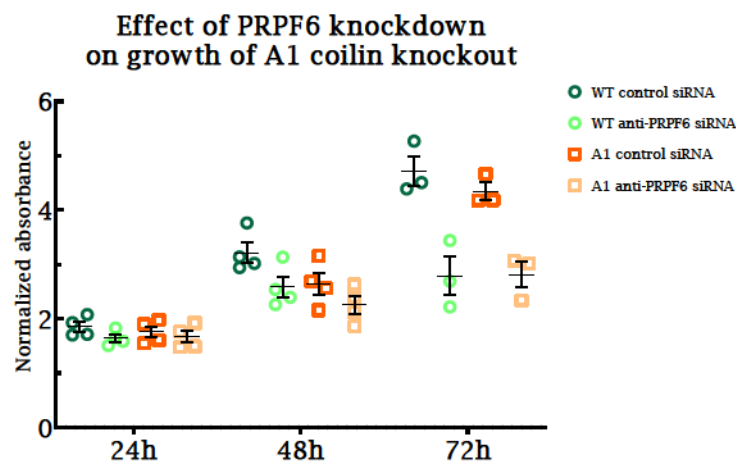
Figure 5.4: Effect of PRPF6 knockdown on growth of A1 coilin knockout compared to the wild type

Cell viability was measured by MTT assay. The growth is displayed as a change in absorbance at 490 nm after 24, 48 and 72 hours after the knockdown. The normalised value was calculated as in Fig. 5.3. The data are represented as individual measurements with mean and SEM bars.

We did not detect any statistically significant difference between the growth of HeLa WT and any other clonal KO cell line under normal culturing conditions (Fig. 5.3). The growth data appear consistent except two measurements – coilin KO A1 and coilin KO B2 absorbance, especially after 48 and 72 hours. They were unexpectedly high. However, we attribute those spikes to imprecise seeding rather than suspecting a meaningful distinction. Other data points of A1 and B2 growth lie within the SEM of the wild type.

Since all the cell lines grew virtually alike, our next step was to create a stressful environment, very much like in the microscopy experiments, to see how absence of coilin affects cell response. We again opted for knockdown of PRPF6 (for representative efficiency of the knockdown see Fig. 5.9a). A sequence of following graphs aims to compare the growth of the individual coilin KO clone proliferation to the WT.

In Fig. 5.4, we could see that there is little difference 24 hours after addition of PRPF6 siRNA not only between the WT and coilin KO A1, but also between the treated and untreated cells. After 48 hours, the difference between PRPF6 knockdown and control cells is becoming more pronounced. At last, the 72 hour data clearly show us that PRPF6 knockdown affects cell proliferation to a significant degree, however, both cell lines reacted very similarly. For quantification, see the resulting Table 5.1.
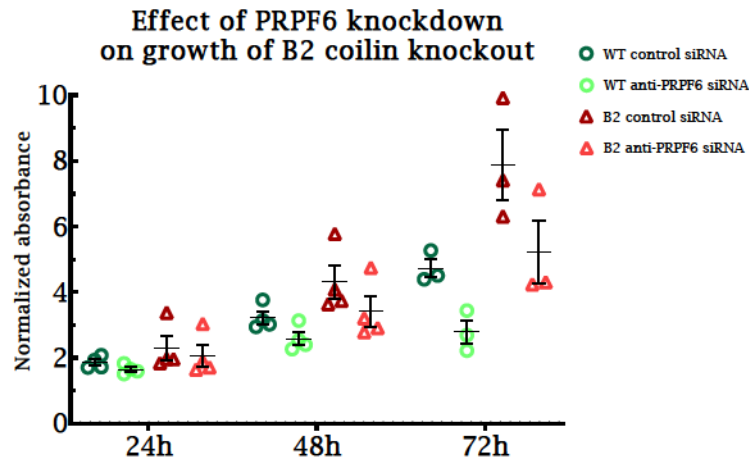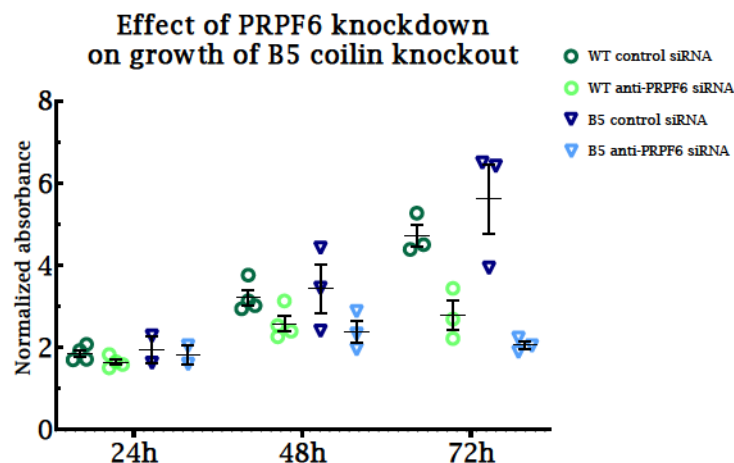
Figure 5.5: Effect of PRPF6 knockdown on growth of B2 coilin knockout compared to the wild type

Cell viability was measured by MTT assay. The growth is displayed as a change in absorbance at 490 nm after 24, 48 and 72 hours after the knockdown. The normalised value was calculated as in Fig. 5.3. The data are represented as individual measurements with mean and SEM bars.

The trend in Fig. 5.5 resembles the previous graph but with the important difference in response of the coilin KO cell line. After 72 hours, it appears that coilin KO B2 experiences lesser drop in proliferation than the WT. Yet the data heterogeneity (SEM bars) seems more prominent as well not allowing for any firm conclusions. For quantification, see the resulting Table 5.1.

Figure 5.6: Effect of PRPF6 knockdown on growth of B5 coilin knockout compared to the wild type

Cell viability was measured by MTT assay. The growth is displayed as a change in absorbance at 490 nm after 24, 48 and 72 hours after the knockdown. The normalised value was calculated as in Fig. 5.3. The data are represented as individual measurements with mean and SEM bars.
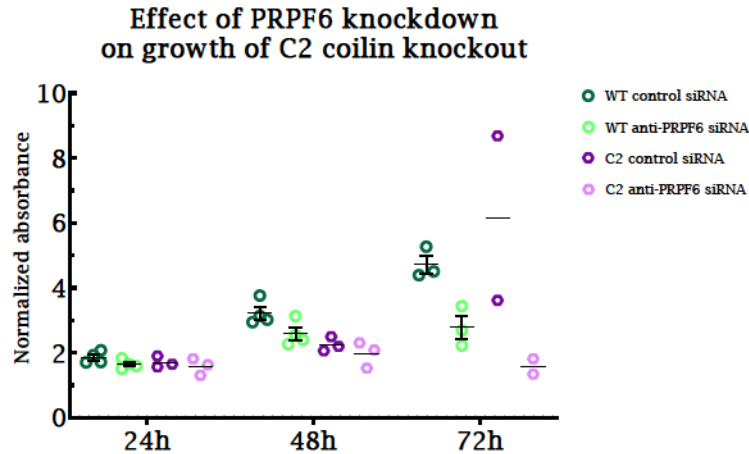
Figure 5.7: Effect of PRPF6 knockdown on growth of C2 coilin knockout compared to the wild type

Cell viability was measured by MTT assay. The growth is displayed as a change in absorbance at 490 nm after 24, 48 and 72 hours after the knockdown. The normalised value was calculated as in Fig. 5.3. The data are represented as individual measurements with mean and SEM bars for the wild type. The data are represented as individual measurements with mean only for C2 coilin knockout cell line.

As to the B5 response, the effect of PRPF6 knockdown is more visible after 48 hour than for A1 or B2 clones (Fig. 5.6). The gap between control cells and treated cells, in case of B5, is conspicuous and bigger than for the WT. Nevertheless, the data are still not entirely harmonious and should be interpreted with care. For quantification, see the resulting Table 5.1. The last investigated clone, C2 coilin KO, was characterised by consistent growth throughout the cell viability examination. Unfortunately, its growth after 72 hours was rather volatile: in the Fig. 5.7, only two data points are shown. Overall, however, there is a certain hint that C2 proliferates slower under snRNP assembly stress conditions.

Time	WT	A1	B2	B5	C2
48h	0.8	0.86 (p=0.16)	0.79 (p=0.48)	0.71 (p=0.11)	0.87 (p=0.39)
72h	0.59	0.65 (p=0.43)	0.66 (p=0.33)	0.39 (p=0.12)	–

Table 5.1: Summarisation of proliferative response to PRPF6 knockdown in different cell lines

Cell viability 48 and 72 hours after the KD is shown. The data are normalised to viability of the cells treated with negative control siRNA. The WT and coilin KO cell lines grew in a similar way. The significance was analysed by t-test.

All in all, the data did not reveal any reliable difference between the wild type and coilin knockout cells. This may serve as an indication that loss of coilin, and, in this way, Cajal bodies, does not sensitise cells for perturbation in snRNP maturation (Table 5.1).

5.3 Coilin knockout cell snRNA level was not significantly different from the wild type

Since there were no revelatory dissimilarities in proliferation, we decided to test whether snRNA levels change in coilin knockout cells. Primarily, we wanted to know if inhibition of snRNP maturation leads to higher degradation or stabilisation of snRNAs in cells lacking coilin. Change in gene expression might reflect a more subtle response and does not necessarily result in a different growth tendency. This time, we tried to evoke the stressed snRNP assembly phenotype by knockdown of either PRPF6, PRPF31 or PRPF8. These proteins are known to result in a similar phenotype but are associated with different snRNPs (for more information see Section 2.1.2). The difference between how the wild type and coilin knockout cell line reacted could give us a clue about the coilin function in the snRNP quality control process.

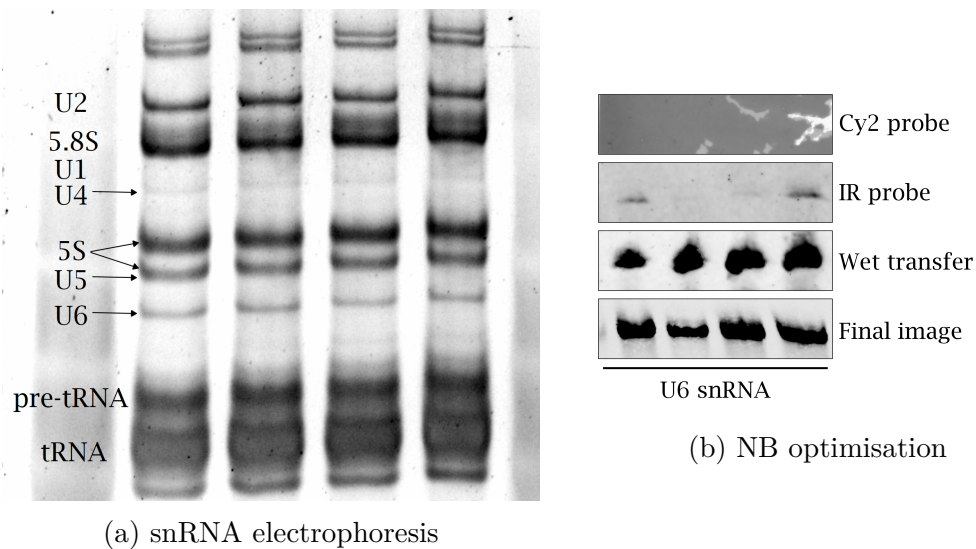
(a) snRNA electrophoresis

(b) NB optimisation

Figure 5.8: Northern blot optimisation

(a) The electrophoresis using TBE/formamide method was done as described in Section 4.2.7. The gel was stained with GelStar as described in Section 4.2.8. Position of the relevant RNAs is indicated. (b) The developed nylon membranes from different experiments are shown. U6 snRNA was detected. The lines (from top to bottom) reflect changes in the NB results upon addition of the specified steps.

The method of choice was Northern blotting (NB) - a reliable method for detection and quantification of changes in RNA level. For our experiments, we used near-infrared fluorescent northern blot analysis. Significant amount of time was spent on figuring out the optimal conditions for snRNA monitoring.

Fig. 5.8b shows a gradual improvement of our Northern blot analysis results. In an attempt to avoid handling radioactive probes for health and convenience reasons, Cyanine2-conjugated probe, typically used for FISH, was tested (Fig. 5.8b (Cy2 probe)). After several unsuccessful trials with RNA detection, full-length U6 double-stranded cDNA was generated and detected by Cyanine2 probe (not shown). It was easier to manipulate with cDNA than with RNA during optimisation steps. Switching to the infrared (IR) hybridisation probes was a key improvement for it substantially reduced the background fluorescence (Fig. 5.8b (IR probe)). Next, the wet-tank transfer method replaced the semi-dry and capillary transfer methods in our protocol (Fig. 5.8b (Wet transfer)). Finally, we adjusted the snRNA electrophoresis according to Masek et al. [2005] so that the bands were of a more favourable for quantification shape, as in Fig. 5.8a and Fig. 5.8b (Final image).

We looked at the tri-snRNP specific snRNAs – U4, U5 and U6. All NB experiments were conducted using B2 coilin KO cell line.

Knockdown of PRPF6 worked very well (Fig. 5.9a). The NB signal (Fig. 5.9b) was sufficient not only for visual assessment but also for quantification. The amount of U4 snRNA was expectedly lower than for U5 or U6 which may partially account for its inconsistent fold change (Fig. 5.9c). In coilin KO cell line, U6 snRNA level was similar to U4 snRNA level. Collectively, the data analysed do not imply any significant difference in how the cells of studied genotypes reacted to the knockdown of PRPF6.

We were sure that the knockdown of PRPF31 was in effect (Fig. 5.10a). From both the NB picture (Fig. 5.10b) and the analysis graph (Fig. 5.10c), it is evident that the cells did not significantly up- or downregulated the snRNA expression, since all the fold changes are consistently close to 1. Along with that, there was an indicative trend in U4: WT appears to have reacted to the knockdown by decreasing amount of the snRNA, whereas coilin KO cell line showed no drop.

In the case of PRPF8 knockdown, its efficiency was not as good as for other proteins (Fig. 5.11a). However, we did not observe any decrease in coilin KO cell line transfectability. Also, the drop in PRPF8 amount was still significant and specific in context of the steady loading control, so we viewed it as sufficient. However, it does not seem that WT and coilin KO react differently (Fig. 5.11b, Fig. 5.11c).
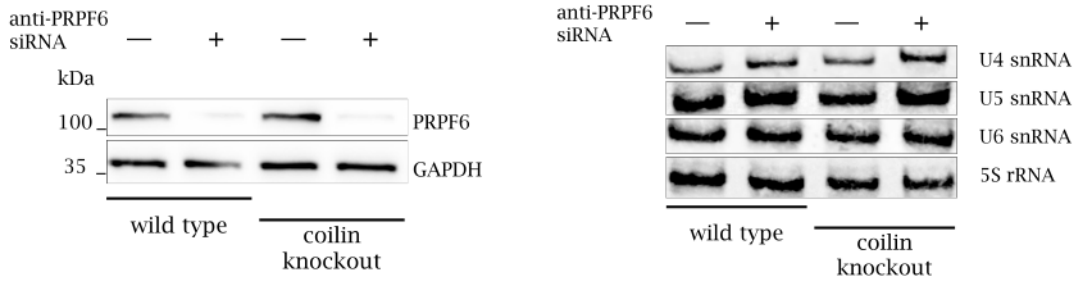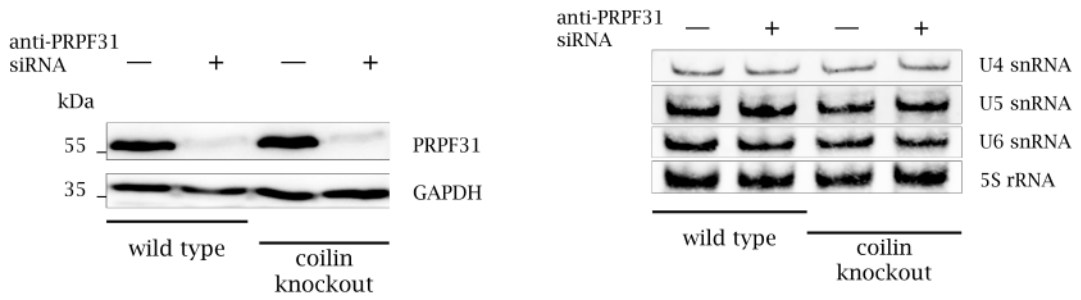
(a) PRPF6 knockdown efficiency

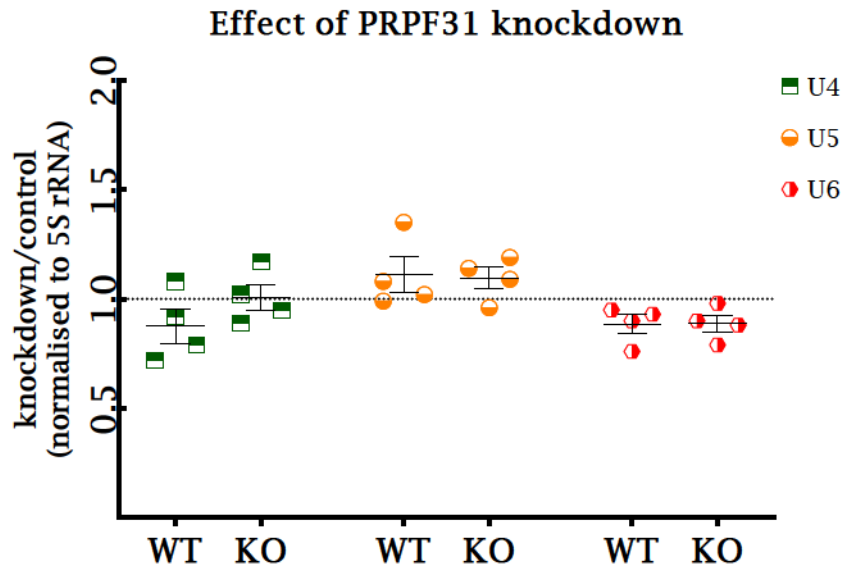(b) Northern blot upon PRPF6 knockdown
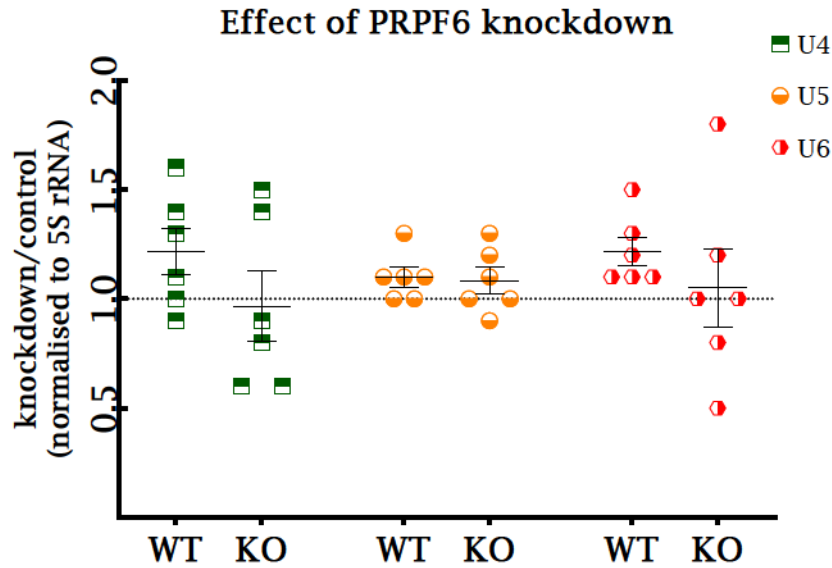
(c) Northern blot analysis. Effect of PRPF6 knockdown

Figure 5.9: PRPF6 knockdown

(a) A representative Western blot detection of PRPF6 is shown. The cells treated with anti-PRPF6 specific siRNA contained markedly less of the protein compared to the negative control siRNA-treated cells. (b) A representative Northern blot detection of tri-snRNP specific snRNAs and 5S rRNA is shown. The anti-PRPF6 siRNA-treated cells appear to accumulate slightly more of U4 and U6 snRNAs. U5 snRNA and 5S rRNA amount do not differ between the cell lines. (c) Analysis of all the performed NBs is shown. The intensities for snRNAs were quantified using Image Lab software and normalised to 5S rRNA. The data points displayed are the fold change of anti-PRPF6 siRNA-treated intensity with respect to the control. None of the differences are significant.
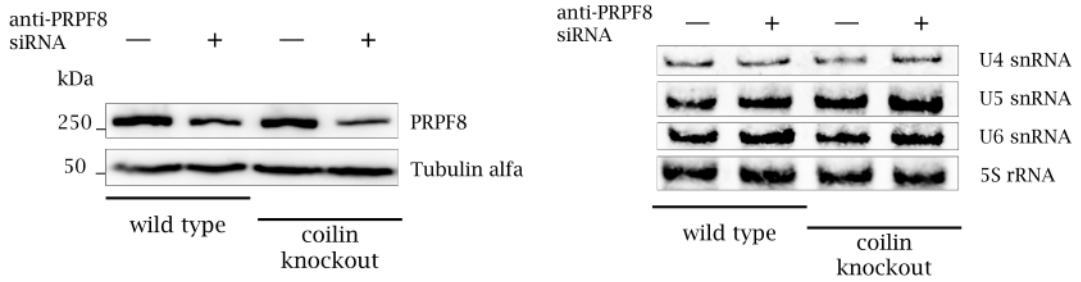
(a) PRPF31 knockdown efficiency
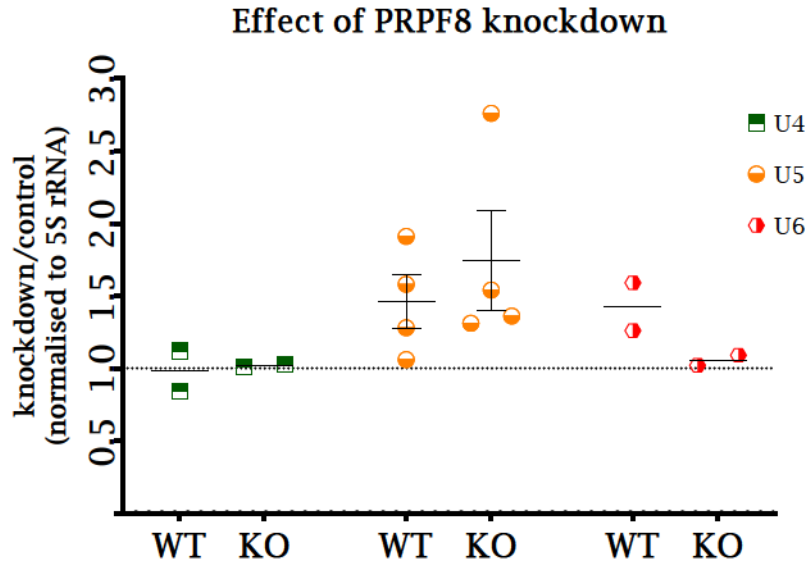

(b) Northern blot upon PRPF31 knockdown

(c) Northern blot analysis. Effect of PRPF31 knockdown

Figure 5.10: PRPF31 knockdown

(a) A representative Western blot detection of PRPF31 is shown. The cells treated with anti-PRPF31 specific siRNA contained markedly less of the protein compared to the negative control siRNA-treated cells. (b) A representative Northern blot detection of tri-snRNP specific snRNAs and 5S rRNA is shown. The amount of snRNAs and 5S rRNA do not differ between the cell lines. (c) Analysis of all the performed NBs is shown. The intensities for snRNAs were quantified using Image Lab software and normalised to 5S rRNA. The data points displayed are the fold change of anti-PRPF31 siRNA-treated intensity with respect to the control. None of the differences are significant.

(a) PRPF8 knockdown efficiency

(b) Northern blot upon PRPF8 knockdown

(c) Northern blot analysis. Effect of PRPF8 knockdown

Figure 5.11: PRPF8 knockdown

(a) A representative Western blot detection of PRPF31 is shown. The cells treated with anti-PRPF8 specific siRNA contained markedly less of the protein compared to the negative control siRNA-treated cells. (b) A representative Northern blot detection of tri-snRNP specific snRNAs and 5S rRNA is shown. The anti-PRPF8 siRNA-treated cells appear to accumulate slightly more of U5 and U6 snRNAs. U4 snRNA and 5S rRNA amount do not differ between the cell lines. (c) Analysis of all the performed NBs is shown. The intensities for snRNAs were quantified using Image Lab software and normalised to 5S rRNA. The data points displayed are the fold change of anti-PRPF8 siRNA-treated intensity with respect to the control. None of the differences are significant.

By the means of Northern blotting, we were unable to determine any statistically significant difference. There were a few trends present but the apparent similarity in the NB pictures for all the knockdowns, as well as the fact that NB is a first of all semi-quantitative method, render them questionable.

As an alternative detection method to NB, we employed reverse transcription coupled with quantitative PCR (RT-qPCR) to monitor changes in snRNA level. We performed multiple experiments with two clonal coilin KO cell lines – B2 and B5. The set-up was the same as for Northern blotting: PRPF6 knockdown was implemented in order to increase concentration of misfolded snRNPs and thus demand for quality control. The efficiency of primers was adequate and was the same for different pairs of primers. The data points displayed in Fig. 5.12 and 5.13 are the fold change of anti-PRPF6 siRNA-treated normalised Ct values with respect to the control. Normalisation was done to 7SK RNA. The significance of WT and KO differences was assessed by t-test.
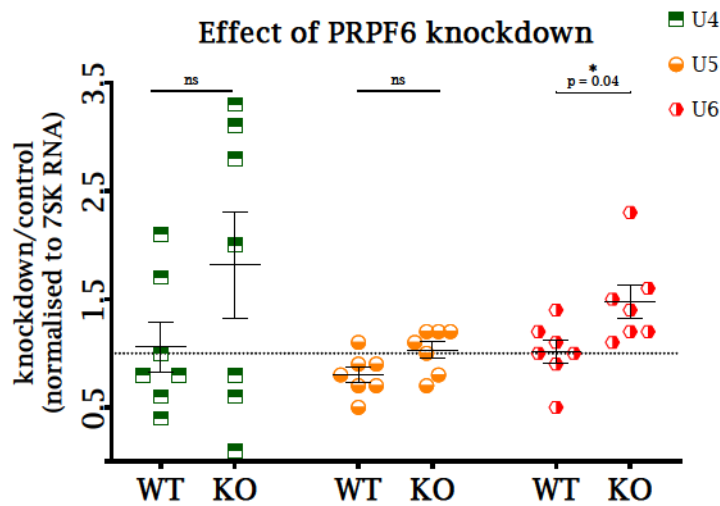

Figure 5.12: RT-qPCR analysis. Effect of PRPF6 knockdown on coilin KO B2

In Fig. 5.12, enormous variation in U4 snRNA expression could be observed, therefore, any possibly present trend is highly unreliable. This snRNA is least abundant out of the three which might have affected accuracy of its quantification. Both U5 and U6 snRNAs expressions were more consistent. Whereas coilin KO and WT response in U5 snRNA steady state level did not differ significantly, U6 snRNA showed a slight increase.
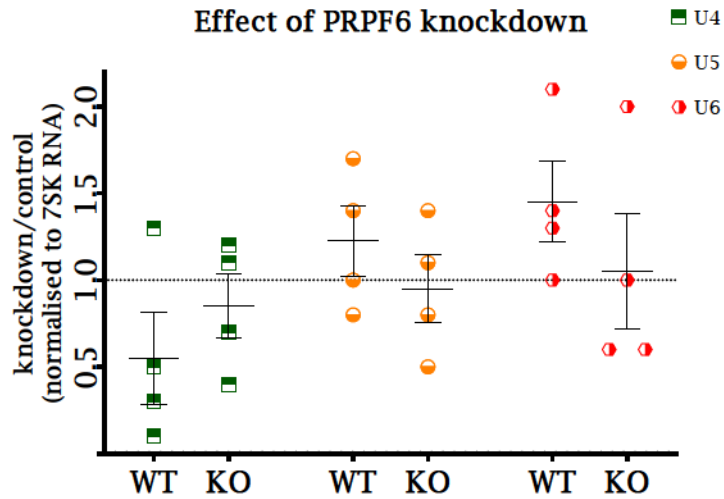
Figure 5.13: RT-qPCR analysis. Effect of PRPF6 knockdown on coilin KO B5

However, none of the patterns were present in B5 coilin KO (Fig. 5.13). All the expression data were fluctuating greatly. It might appear that, in coilin knock-out, expression of U5 and U6 snRNA insignificantly declined upon the PRPF6 knockdown.

All in all, the data acquired from the qPCR analyses from both clones were untrustworthy due to high variation, as well as contradicting the NB results.

6. Discussion

Coilin is omnipresent in many different species, as well as being expressed in majority of human cell types (Carmo-Fonseca et al. [1993], Liu et al. [2009], Tucker et al. [2001], Strzelecka et al. [2010], Thul et al. [2017]). It was found to associate with numerous entities, including DNA, RNA and proteins. Many of them are tightly connected to snRNP biogenesis (Machyna et al. [2014], Smith et al. [1995], Enwerem et al. [2014], Boulon et al. [2004], Xu et al. [2005], Novotny et al. [2015]). Coilin gives rise to the Cajal body, most probably via its ability to self-interact and to "glue" the Cajal body components together (Machyna et al. [2015]).

After more than 25 years of studying coilin, researchers are still not sure what its molecular function is. There is also relatively little information in the literature on snRNP stability *in vivo*. Therefore, we decided to address snRNP-related function of coilin. For this purpose, we worked with coilin knockout cell line under conditions of strained snRNP biogenesis caused by knockdown of pre-mRNA processing factors. Our main expectation was to see a phenotypic difference in how coilin KO reacts to the KD. Three types of analysis were carried out: visual, proliferative and snRNA steady state level.

In concordance with Novotny et al. [2015], we observed explicit accumulation of snRNPs in the CBs of HeLa WT upon the PRPF6 KD (Fig. 5.1). Presumably, "Final maturation steps" (Section 2.1.2) were affected by the KD, since PRPF6 is required for tri-snRNP formation *in vivo*. The microphotographs also show that U5 snRNP is not fully localised to the bodies and remains in the nucleoplasm to a visibly greater extent than U4 and U2 snRNP. This agrees well with what is already known about PRPF6 KD effect on the WT cells – targeting of U4/U6 di-snRNP to the CBs, but not U5 snRNPs (Schaffert et al. [2004]). The snRNPs were sequestered in the CBs, apparently, to prevent the faulty particles from continuing up the biogenesis pathway and taking part in splicing reaction. This observation points to the possible role of CBs in snRNP quality control as suggested previously (Novotny et al. [2015], Schaffert et al. [2004]). Interestingly, Nesic et al. [2004] showed that immediately after U2 snRNP completes its maturation, the particles are released from the CB and localise in the nuclear speckles. We did not observe this upon the KD of the tri-snRNP specific protein – PRPF6. U2 snRNA retention was repeatedly detected in the CB which could mean that PRPF6 depletion affects U2 snRNP biogenesis too. Most probably, the 12S U2 snRNP particles, intermediates of the U2 snRNP assembly, accumulate in the CBs. The retention likely takes place after the re-import into the nucleus, and also prior to binding of SF3A, as indicated by Tanackovic and Kramer [2005]. This fact, however, contradicts the findings of Novotny et al. [2015] where U2 snRNA did not localise to the CB upon KD of PRPF6, SART3 or PRPF8. Therefore, our observation might either indicate a more complex interplay between the assembly of different snRNP particles than previously thought or be a mere artefact of the investigative procedure inaccuracy.

Predictably, no snRNP accumulation was visible in the coilin KO cells upon the PRPF6 KD (Fig. 5.2). The cells were seemingly unable to sequester stalled snRNPs in absence of coilin as was the case with coilin knockout mice in Tucker

et al. [2001]. In the mentioned publication, ectopic expression of normal coilin led to re-appearance of CBs, hence coilin is required for recruitment of specific components and the quality control function of the CB. Another thing to take notice of is presence of cytoplasmic signal for U4 snRNA – could those dots represent U-bodies? Does it then suggest that the U body–P body pathway is involved in dealing with misfolded U4 snRNP? It has been suggested that U body and P-bodies might contribute to spliceosomal constituent assembly (Roithova et al. [2020], Lee et al. [2009]). In order to test this hypothesis, another FISH experiment would be required where we stain a marker of U bodies (SMN or GEMIN3) or P bodies (DCP1A). On the other hand, the bright cytoplasmic foci might be nothing more than a staining artefact since no other snRNA co-localises there.

We hypothesised that, upon PRPF6 KD, the coilin KO cells should be under high physiological stress due to increased concentration of misfolded snRNPs. Moreover, they could not store those defective particles in one place to prevent them from interfering with other nuclear processes due to absence of the CBs. Reduced cell proliferation and increased apoptosis would be a logical response to such a considerable burden. Therefore, cell viability was examined by MTT assay.

However, first of all, we looked at the culture growth under normal conditions, as described in Section 4.2.1. HeLa cells with canonical CBs had been reported to generate snRNPs and perform splicing more efficiently than coilin knockdown cell line (Whittom et al. [2008]), and therefore might have a greater proliferation potential. Unfortunately, our finding could not be interpreted in this way – there was no statistically significant difference in growth of WT versus coilin KO cell lines under physiological conditions (Fig. 5.3). One possible reason for our observation is excessive sub-culturing of coilin KO cells, even though we tried to limit its effect by assessing several clones. Possibly, the cells adapted to surviving in culture without coilin. Another explanation could be that, under normal growth conditions in HeLa cells, CB-mediated high snRNP maturation and quality control rate are not imperative for proliferation. Indeed, in *Drosophila* and *Arabidopsis* neither coilin nor CB are essential for cell viability (Liu et al. [2009], Collier et al. [2006]) On the other hand, coilin depletion was demonstrated to inhibit proliferation most probably by limiting the rate of processes important for cell growth and/or division (Lemm et al. [2006]).

Next, we implemented PRPF6 knockdown. Overall, its effect on the WT and coilin KO cell line was very similar (Table 5.1). Both cell lines reacted with roughly 20% decrease in cell viability 48 h after the knockdown and 40 to 60% drop after 72 h. Any possible difference 72 h after the KD was insignificant. Clear absence of any coilin KO-dependent proliferative response was rather surprising. It did not agree well with earlier findings that coilin KO have difficulty generating snRNPs and thus have reduced splicing potential (Whittom et al. [2008]). On the other hand, there are reports of phenotypically normal human coilin KO cell line with respect to hTR metabolism which is also thought to be CB-related (Chen et al. [2015]).

Another thing to take into account was that HeLa cells could deal with the spike in flawed snRNPs via some backup or offset mechanism. Among those mechanisms are under- or overexpression of snRNP components (snRNA or protein)

and non-coilin assembly-assisting components of the CB (maturation, trafficking, recycling factors, etc. – e.g. SART3). Here, we decided to address U4, U5 and U6 snRNA steady state levels by Northern blotting and qRT-PCR.

Three proteins were selected for the knockdown so that we target different maturation steps. PRPF31 is required for di-snRNP formation meaning that its absence should result in surge of immature U4 and U6 snRNPs, as well as faulty di-snRNPs. It is also reported to prevent U5 snRNP and U4/U6 di-snRNP interaction (Schaffert et al. [2004]). PRPF8 is a central U5 snRNP-specific protein. Without it, tri-snRNP formation is blocked resulting in di-snRNP and defected U5 snRNP concentration increase (Liu et al. [2006], Novotny et al. [2015]). Lastly, PRPF6 interacts with U5 snRNA, PRPF31 and PRPF3. By this, it brings together di-snRNP and U5 snRNP and enables the tri-snRNP formation. PRPF6 KD is known to result in a dramatic drop in tri-snRNP concentration (more than 80%), hence in accumulation of its precursors (Schaffert et al. [2004], Liu et al. [2006]). By determining the responses of coilin KO to perturbation at certain stages, we hoped to elucidate what maturation steps coilin is most important for.

Upon PRPF6 knockdown, a certain, albeit insignificant, tendency in U6 and U4 snRNAs stability was present (Fig. 5.9c). Hypothetically, a slight decrease in those snRNAs could suggest that coilin facilitates stabilisation of the di-snRNP, most probably with the aid of SART3. By doing so, it would create an opportunity for snRNP remodelling – recycling of the intact parts and degradation of the faulty ones. On the other hand, this accumulation can be transient and, in a long run, assist in recruitment of the degradation machinery to the defected particles. Alternatively, upscaling the snRNA amounts in the CB could readdress the balance and make up for insufficient amount of tri-snRNPs upon the KD. Our RT-qPCR results, however, show a completely opposite trend (Fig. 5.12) when PRPF6 knockdown was in place. For U6 and U4 snRNAs we observed a slight increase. This, in turn, could suggest that coilin facilitates more efficient di- and tri-snRNP precursors degradation and recycling, so that they do not interfere with the metabolism of complete particles. It has been reported before that when the tri-snRNP formation is inhibited, U5 snRNP distribution in the nucleus remains unchanged (Schaffert et al. [2004]). Novotny et al. [2015] observed U5 snRNP accumulation only upon PRPF8 KD, but not PRPF6. Here, we showed a steady U5 snRNA fold changes by NB and RT-qPCR which agrees with those findings (Fig. 5.9c, 5.12 and 5.13).

Regarding the depletion of PRPF31, we used the same siRNA design as Schaffert et al. [2004], Table 4.1. It has been demonstrated that PRPF31 KD affects cell growth even more than PRPF6 KD – 45% and 30% respectively. Because of this, we expected a more pronounce difference in snRNA levels in cells without coilin. In WT cells, though, the absence of a clear snRNA response is in unison with Schaffert et al. [2004] and Makarova et al. [2002].

In literature, PRPF8 deficiency is generally connected to the maturation of U5 snRNP, even though it was also shown to affect U4 and U6 snRNPs. Our experiments showed that in both studied cell lines U5 snRNA was upregulated confirming the finding by high-content microscopy (Novotny et al. [2015]). The fact that coilin KO cells reacted in the same way suggests that this protein does not play a crucial role in managing U5 snRNP-related burden and that its quality control might proceed without it. Nevertheless, further experiments are needed.

Trends aside, lack of a significant shift in snRNA concentration in coilin-deficient cells upon a spike in the amount of incomplete snRNP particles means that neither stabilisation nor degradation of snRNAs take place in the Cajal body. With this conclusion, it might be tempting to speculate that the U4 specific cytoplasmic foci from Fig. 5.2, if related to U body-P body pathway, might be utilised instead or as a partial subtitute for CBs. By having alternative cytoplasmic hubs which brings various spliceosomal components together, cell devoid of coilin could harmonise snRNP asssembly. Although this could serve as a possible explanation for the acquired results, it remains a mere speculation until further research is done.

In light of all mentioned above, it could also be interesting to analyse snoRNA steady state levels in absence of coilin since they were shown to shuttle through the CBs (Machyna et al. [2014]). At the same time, we consider follow-up experiments in models which express unusually high amounts of spliceosome components (e.g. retina cells) and might be more easily sensitised for perturbation in snRNP maturation without coilin. Simultaneous depletion of coilin by siRNA-mediated knockdown and expression of the altered coilin constructs might help reduce the clonal effect. Another valuable insight could be gained by understanding whether coilin becomes essential upon strained snRNP assembly in *Drosophila melanogaster* or *Arabidopsis thaliana*.

Summarising, in this thesis we removed coilin and inhibited snRNP biogenesis, as we believed it was the best way to understand the fate of immature snRNPs normally sequestered in CBs. At the same time, we raised questions on whether coilin is a truly influential player in quality control of incomplete or faulty snRNP particles. Other experiments ought to be performed to elucidate or rule out coilin's part in the final steps of snRNP assembly in *Homo sapiens*. After all, coilin KO is an embryonic lethal mutation in *Mus musculus*. Therefore, the precise biological and even species-specific function and significance of coilin remains imperfectly understood, and thus need to be studied further.

Conclusion

The thesis has searched for the role of coilin in snRNP quality control. Coilin was reporter to interact with numerous snRNP biogenesis participants, and to serve as a scaffold for the Cajal body – a suggested snRNP maturation site. This work has proposed an assessment of human coilin knockout cell line phenotype to elucidate how important coilin, and, by extension, Cajal bodies, are for spliceosomal assembly and function. By comparing a coilin-deficient cell line to the wild type cell line, coilin role was evaluated visually, in terms of cell viability and snRNA steady levels under the conditions of strained snRNP assembly.

It has been determined that knockout cells are unable to sequester misfolded snRNP particles confirming that coilin is crucial for the sequestration. Next, we have shown that cell proliferation was not significantly affected by absence of coilin neither under normal culturing conditions nor under stressful conditions. Similarly, it appears that coilin deficiency does not significantly alter stability of snRNA. In the future, we intend to investigate coilin function in a different biological model, e.g. human retinal organoids, in *Drosophila melanogaster* or *Arabidopsis thaliana*, as well as trying to target other steps of snRNP maturation.

Bibliography

T. Achsel, H. Brahms, B. Kastner, A. Bachi, M. Wilm, and R. Luhrmann. A doughnut-shaped heteromer of human sm-like proteins binds to the 3'-end of u6 snrna, thereby facilitating u4/u6 duplex formation in vitro. *EMBO J*, 18(20): 5789–802, 1999. ISSN 0261-4189 (Print) 0261-4189 (Linking). doi: 10.1093/emboj/18.20.5789. URL `https://www.ncbi.nlm.nih.gov/pubmed/10523320`.

L. E. Andrade, E. K. Chan, I. Raska, C. L. Peebles, G. Roos, and E. M. Tan. Human autoantibody to a novel protein of the nuclear coiled body: immunological characterization and cdna cloning of p80-coilin. *J Exp Med*, 173(6):1407–19, 1991. ISSN 0022-1007 (Print) 0022-1007. doi: 10.1084/jem.173.6.1407.

L. E. Andrade, E. M. Tan, and E. K. Chan. Immunocytochemical analysis of the coiled body in the cell cycle and during cell proliferation. *Proc Natl Acad Sci U S A*, 90(5):1947–51, 1993. ISSN 0027-8424 (Print) 0027-8424 (Linking). doi: 10.1073/pnas.90.5.1947. URL `https://www.ncbi.nlm.nih.gov/pubmed/8446613`.

P. Askjaer, A. Bachi, M. Wilm, F. R. Bischoff, D. L. Weeks, V. Ogniewski, M. Ohno, C. Niehrs, J. Kjems, I. W. Mattaj, and M. Fornerod. Rangtp-regulated interactions of crm1 with nucleoporins and a shuttling dead-box helicase. *Mol Cell Biol*, 19(9):6276–85, 1999. ISSN 0270-7306 (Print) 0270-7306 (Linking). doi: 10.1128/MCB.19.9.6276. URL `https://www.ncbi.nlm.nih.gov/pubmed/10454574`.

John F. Gesteland Raymond F. Cech Thomas Atkins. *RNA worlds : from life's origins to diversity in gene regulation.* Cold Spring Harbor Laboratory Press, Cold Spring Harbor, N.Y., 2011. ISBN 9780879699468 0879699469.

R. Bai, R. Wan, C. Yan, J. Lei, and Y. Shi. Structures of the fully assembled saccharomyces cerevisiae spliceosome before activation. *Science*, 360(6396):1423–1429, 2018. ISSN 1095-9203 (Electronic) 0036-8075 (Linking). doi: 10.1126/science.aau0325. URL `https://www.ncbi.nlm.nih.gov/pubmed/29794219`.

J. Bizarro, M. Dodre, A. Huttin, B. Charpentier, F. Schlotter, C. Branlant, C. Verheggen, S. Massenet, and E. Bertrand. Nufip and the hsp90/r2tp chaperone bind the smn complex and facilitate assembly of u4-specific proteins. *Nucleic Acids Res*, 43(18):8973–89, 2015. ISSN 1362-4962 (Electronic) 0305-1048 (Linking). doi: 10.1093/nar/gkv809. URL `https://www.ncbi.nlm.nih.gov/pubmed/26275778`.

S. Boulon, C. Verheggen, B. E. Jady, C. Girard, C. Pescia, C. Paul, J. K. Ospina, T. Kiss, A. G. Matera, R. Bordonne, and E. Bertrand. Phax and crm1 are required sequentially to transport u3 snorna to nucleoli. *Mol Cell*, 16(5):777–87, 2004. ISSN 1097-2765 (Print) 1097-2765 (Linking). doi: 10.1016/j.molcel.2004.11.013. URL `https://www.ncbi.nlm.nih.gov/pubmed/15574332`.

E. M. Bradbury, S. E. Danby, H. W. Rattle, and V. Giancotti. Studies on the role and mode of operation of the very-lysine-rich histone h1 (f1) in eukaryote

chromatin. histone h1 in chromatin and in h1 - dna complexes. *Eur J Biochem*, 57(1):97–105, 1975. ISSN 0014-2956 (Print) 0014-2956 (Linking). doi: 10.1111/ j.1432-1033.1975.tb02280.x. URL `https://www.ncbi.nlm.nih.gov/pubmed/ 1175645`.

C. Branlant, A. Krol, J. P. Ebel, E. Lazar, B. Haendler, and M. Jacob. U2 rna shares a structural domain with u1, u4, and u5 rnas. *EMBO J*, 1(10): 1259–65, 1982. ISSN 0261-4189 (Print) 0261-4189 (Linking). URL `https: //www.ncbi.nlm.nih.gov/pubmed/6202507`.

C. Carissimi, J. Baccon, M. Straccia, P. Chiarella, A. Maiolica, A. Sawyer, J. Rappsilber, and L. Pellizzoni. Unrip is a component of smn complexes active in snrnp assembly. *FEBS Lett*, 579(11):2348–54, 2005. ISSN 0014-5793 (Print) 0014-5793 (Linking). doi: 10.1016/j.febslet.2005.03.034. URL `https://www.ncbi.nlm.nih.gov/pubmed/15848170`.

M. Carmo-Fonseca, J. Ferreira, and A. I. Lamond. Assembly of snrnp-containing coiled bodies is regulated in interphase and mitosis–evidence that the coiled body is a kinetic nuclear structure. *J Cell Biol*, 120(4):841–52, 1993. ISSN 0021-9525 (Print) 0021-9525 (Linking). doi: 10.1083/jcb.120.4.841. URL `https: //www.ncbi.nlm.nih.gov/pubmed/7679389`.

C. Charenton, M. E. Wilkinson, and K. Nagai. Mechanism of 5' splice site transfer for human spliceosome activation. *Science*, 364(6438):362–367, 2019. ISSN 1095-9203 (Electronic) 0036-8075 (Linking). doi: 10.1126/science.aax3289. URL `https://www.ncbi.nlm.nih.gov/pubmed/30975767`.

T. Chen, F. M. Boisvert, D. P. Bazett-Jones, and S. Richard. A role for the gsg domain in localizing sam68 to novel nuclear structures in cancer cell lines. *Mol Biol Cell*, 10(9):3015–33, 1999. ISSN 1059-1524 (Print) 1059-1524 (Linking). doi: 10.1091/mbc.10.9.3015. URL `https://www.ncbi.nlm.nih.gov/pubmed/ 10473643`.

Y. Chen, Z. Deng, S. Jiang, Q. Hu, H. Liu, Z. Songyang, W. Ma, S. Chen, and Y. Zhao. Human cells lacking coilin and cajal bodies are proficient in telomerase assembly, trafficking and telomere maintenance. *Nucleic Acids Res*, 43(1):385–95, 2015. ISSN 1362-4962 (Electronic) 0305-1048 (Linking). doi: 10.1093/nar/ gku1277. URL `https://www.ncbi.nlm.nih.gov/pubmed/25477378`.

S. Collier, A. Pendle, K. Boudonck, T. van Rij, L. Dolan, and P. Shaw. A distant coilin homologue is required for the formation of cajal bodies in arabidopsis. *Mol Biol Cell*, 17(7):2942–51, 2006. ISSN 1059-1524 (Print) 1059-1524 (Linking). doi: 10.1091/mbc.e05-12-1157. URL `https://www.ncbi.nlm.nih.gov/ pubmed/16624863`.

R. Das, K. Dufu, B. Romney, M. Feldt, M. Elenko, and R. Reed. Functional coupling of rnap ii transcription to spliceosome assembly. *Genes Dev*, 20(9): 1100–9, 2006. ISSN 0890-9369 (Print) 0890-9369 (Linking). doi: 10.1101/gad. 1397406. URL `https://www.ncbi.nlm.nih.gov/pubmed/16651655`.

S. Egloff, S. A. Szczepaniak, M. Dienstbier, A. Taylor, S. Knight, and S. Murphy. The integrator complex recognizes a new double mark on the rna polymerase ii carboxyl-terminal domain. *J Biol Chem*, 285(27):20564–9, 2010. ISSN 1083-351X (Electronic) 0021-9258 (Linking). doi: 10.1074/jbc.M110.132530. URL `https://www.ncbi.nlm.nih.gov/pubmed/20457598`.

II Enwerem, V. Velma, H. J. Broome, M. Kuna, R. A. Begum, and M. D. Hebert. Coilin association with box c/d scarna suggests a direct role for the cajal body marker protein in scarnp biogenesis. *Biol Open*, 3(4):240–9, 2014. ISSN 2046-6390 (Print) 2046-6390 (Linking). doi: 10.1242/bio.20147443. URL `https://www.ncbi.nlm.nih.gov/pubmed/24659245`.

U. Fischer, C. Englbrecht, and A. Chari. Biogenesis of spliceosomal small nuclear ribonucleoproteins. *Wiley Interdiscip Rev RNA*, 2(5):718–31, 2011. ISSN 1757-7012 (Electronic) 1757-7004 (Linking). doi: 10.1002/wrna.87. URL `https://www.ncbi.nlm.nih.gov/pubmed/21823231`.

M. R. Frey and A. G. Matera. Rna-mediated interaction of cajal bodies and u2 snrna genes. *J Cell Biol*, 154(3):499–509, 2001. ISSN 0021-9525 (Print) 0021-9525 (Linking). doi: 10.1083/jcb.200105084. URL `https://www.ncbi.nlm.nih.gov/pubmed/11489914`.

M. R. Frey, A. D. Bailey, A. M. Weiner, and A. G. Matera. Association of snrna genes with coiled bodies is mediated by nascent snrna transcripts. *Curr Biol*, 9(3):126–35, 1999. ISSN 0960-9822 (Print) 0960-9822 (Linking). doi: 10.1016/s0960-9822(99)80066-9. URL `https://www.ncbi.nlm.nih.gov/pubmed/10021385`.

W. P. Galej, C. Oubridge, A. J. Newman, and K. Nagai. Crystal structure of prp8 reveals active site cavity of the spliceosome. *Nature*, 493(7434):638–43, 2013. ISSN 1476-4687 (Electronic) 0028-0836 (Linking). doi: 10.1038/nature11843. URL `https://www.ncbi.nlm.nih.gov/pubmed/23354046`.

P. Ganot, B. E. Jady, M. L. Bortolin, X. Darzacq, and T. Kiss. Nucleolar factors direct the 2'-o-ribose methylation and pseudouridylation of u6 spliceosomal rna. *Mol Cell Biol*, 19(10):6906–17, 1999. ISSN 0270-7306 (Print) 0270-7306 (Linking). doi: 10.1128/MCB.19.10.6906. URL `https://www.ncbi.nlm.nih.gov/pubmed/10490628`.

C. Grimm, A. Chari, J. P. Pelz, J. Kuper, C. Kisker, K. Diederichs, H. Stark, H. Schindelin, and U. Fischer. Structural basis of assembly chaperone- mediated snrnp formation. *Mol Cell*, 49(4):692–703, 2013. ISSN 1097-4164 (Electronic) 1097-2765 (Linking). doi: 10.1016/j.molcel.2012.12.009. URL `https://www.ncbi.nlm.nih.gov/pubmed/23333303`.

J. Gu, G. Shumyatsky, N. Makan, and R. Reddy. Formation of 2',3'-cyclic phosphates at the 3' end of human u6 small nuclear rna in vitro. identification of 2',3'-cyclic phosphates at the 3' ends of human signal recognition particle and mitochondrial rna processing rnas. *J Biol Chem*, 272(35):21989–93, 1997. ISSN 0021-9258 (Print) 0021-9258 (Linking). doi: 10.1074/jbc.272.35.21989. URL `https://www.ncbi.nlm.nih.gov/pubmed/9268336`.

M. Hallais, F. Pontvianne, P. R. Andersen, M. Clerici, D. Lener, H. Benbahouche Nel, T. Gostan, F. Vandermoere, M. C. Robert, S. Cusack, C. Verheggen, T. H. Jensen, and E. Bertrand. Cbc-ars2 stimulates 3'-end maturation of multiple rna families and favors cap-proximal processing. *Nat Struct Mol Biol*, 20(12):1358–66, 2013. ISSN 1545-9985 (Electronic) 1545-9985 (Linking). doi: 10.1038/nsmb.2720. URL https://www.ncbi.nlm.nih.gov/pubmed/24270878.

J. Hamm and I. W. Mattaj. An abundant u6 snrnp found in germ cells and embryos of xenopus laevis. *EMBO J*, 8(13):4179–87, 1989. ISSN 0261-4189 (Print) 0261-4189 (Linking). URL https://www.ncbi.nlm.nih.gov/pubmed/2531660.

S. M. Hearst, A. S. Gilder, S. S. Negi, M. D. Davis, E. M. George, A. A. Whittom, C. G. Toyota, A. Husedzinovic, O. J. Gruss, and M. D. Hebert. Cajal-body formation correlates with differential coilin phosphorylation in primary and transformed cell lines. *J Cell Sci*, 122(Pt 11):1872–81, 2009. ISSN 0021-9533 (Print) 0021-9533 (Linking). doi: 10.1242/jcs.044040. URL https://www.ncbi.nlm.nih.gov/pubmed/19435804.

M. D. Hebert and A. G. Matera. Self-association of coilin reveals a common theme in nuclear body localization. *Mol Biol Cell*, 11(12):4159–71, 2000. ISSN 1059-1524 (Print) 1059-1524 (Linking). doi: 10.1091/mbc.11.12.4159. URL https://www.ncbi.nlm.nih.gov/pubmed/11102515.

M. D. Hebert, P. W. Szymczyk, K. B. Shpargel, and A. G. Matera. Coilin forms the bridge between cajal bodies and smn, the spinal muscular atrophy protein. *Genes Dev*, 15(20):2720–9, 2001. ISSN 0890-9369 (Print) 0890-9369 (Linking). doi: 10.1101/gad.908401. URL https://www.ncbi.nlm.nih.gov/pubmed/11641277.

M. D. Hebert, K. B. Shpargel, J. K. Ospina, K. E. Tucker, and A. G. Matera. Coilin methylation regulates nuclear body formation. *Dev Cell*, 3(3):329–37, 2002. ISSN 1534-5807 (Print) 1534-5807 (Linking). doi: 10.1016/s1534-5807(02)00222-8. URL https://www.ncbi.nlm.nih.gov/pubmed/12361597.

R. W. Henry, V. Mittal, B. Ma, R. Kobayashi, and N. Hernandez. Snap19 mediates the assembly of a functional core promoter complex (snapc) shared by rna polymerases ii and iii. *Genes Dev*, 12(17):2664–72, 1998. ISSN 0890-9369 (Print) 0890-9369 (Linking). doi: 10.1101/gad.12.17.2664. URL https://www.ncbi.nlm.nih.gov/pubmed/9732265.

N. Hernandez. Formation of the 3' end of u1 snrna is directed by a conserved sequence located downstream of the coding region. *EMBO J*, 4(7):1827–37, 1985. ISSN 0261-4189 (Print) 0261-4189 (Linking). URL https://www.ncbi.nlm.nih.gov/pubmed/2411548.

N. Hernandez. Small nuclear rna genes: a model system to study fundamental mechanisms of transcription. *J Biol Chem*, 276(29):26733–6, 2001. ISSN 0021-9258 (Print) 0021-9258 (Linking). doi: 10.1074/jbc.R100032200. URL https://www.ncbi.nlm.nih.gov/pubmed/11390411.

N. Hernandez and A. M. Weiner. Formation of the 3' end of u1 snrna requires compatible snrna promoter elements. *Cell*, 47(2):249–58, 1986. ISSN 0092-8674 (Print) 0092-8674 (Linking). doi: 10.1016/0092-8674(86)90447-2. URL `https://www.ncbi.nlm.nih.gov/pubmed/3768956`.

M. J. Hicks, C. R. Yang, M. V. Kotlajich, and K. J. Hertel. Linking splicing to pol ii transcription stabilizes pre-mrnas and influences splicing patterns. *PLoS Biol*, 4(6):e147, 2006. ISSN 1545-7885 (Electronic) 1544-9173 (Linking). doi: 10.1371/journal.pbio.0040147. URL `https://www.ncbi.nlm.nih.gov/pubmed/16640457`.

J. Huber, U. Cronshagen, M. Kadokura, C. Marshallsay, T. Wada, M. Sekine, and R. Luhrmann. Snurportin1, an m3g-cap-specific nuclear import receptor with a novel domain structure. *EMBO J*, 17(14):4114–26, 1998. ISSN 0261-4189 (Print) 0261-4189 (Linking). doi: 10.1093/emboj/17.14.4114. URL `https://www.ncbi.nlm.nih.gov/pubmed/9670026`.

J. Huber, A. Dickmanns, and R. Luhrmann. The importin-beta binding domain of snurportin1 is responsible for the ran- and energy-independent nuclear import of spliceosomal u snrnps in vitro. *J Cell Biol*, 156(3):467–79, 2002. ISSN 0021-9525 (Print) 0021-9525 (Linking). doi: 10.1083/jcb.200108114. URL `https://www.ncbi.nlm.nih.gov/pubmed/11815630`.

C. Isaac, Y. Yang, and U. T. Meier. Nopp140 functions as a molecular link between the nucleolus and the coiled bodies. *J Cell Biol*, 142(2):319–29, 1998. ISSN 0021-9525 (Print) 0021-9525 (Linking). doi: 10.1083/jcb.142.2.319. URL `https://www.ncbi.nlm.nih.gov/pubmed/9679133`.

A. M. Ishov, A. G. Sotnikov, D. Negorev, O. V. Vladimirova, N. Neff, T. Kamitani, E. T. Yeh, 3rd Strauss, J. F., and G. G. Maul. Pml is critical for nd10 formation and recruits the pml-interacting protein daxx to this nuclear structure when modified by sumo-1. *J Cell Biol*, 147(2):221–34, 1999. ISSN 0021-9525 (Print) 0021-9525 (Linking). doi: 10.1083/jcb.147.2.221. URL `https://www.ncbi.nlm.nih.gov/pubmed/10525530`.

E. Izaurralde, J. Lewis, C. Gamberi, A. Jarmolowski, C. McGuigan, and I. W. Mattaj. A cap-binding protein complex mediating u snrna export. *Nature*, 376(6542):709–12, 1995. ISSN 0028-0836 (Print) 0028-0836 (Linking). doi: 10.1038/376709a0. URL `https://www.ncbi.nlm.nih.gov/pubmed/7651522`.

H. Izumi, A. McCloskey, K. Shinmyozu, and M. Ohno. p54nrb/nono and psf promote u snrna nuclear export by accelerating its export complex assembly. *Nucleic Acids Res*, 42(6):3998–4007, 2014. ISSN 1362-4962 (Electronic) 0305-1048 (Linking). doi: 10.1093/nar/gkt1365. URL `https://www.ncbi.nlm.nih.gov/pubmed/24413662`.

E. Y. Jacobs, M. R. Frey, W. Wu, T. C. Ingledue, T. C. Gebuhr, L. Gao, W. F. Marzluff, and A. G. Matera. Coiled bodies preferentially associate with u4, u11, and u12 small nuclear rna genes in interphase hela cells but not with u6 and u7 genes. *Mol Biol Cell*, 10(5):1653–63, 1999. ISSN 1059-1524 (Print) 1059-1524 (Linking). doi: 10.1091/mbc.10.5.1653. URL `https://www.ncbi.nlm.nih.gov/pubmed/10233169`.

B. E. Jady, X. Darzacq, K. E. Tucker, A. G. Matera, E. Bertrand, and T. Kiss. Modification of sm small nuclear rnas occurs in the nucleoplasmic cajal body following import from the cytoplasm. *EMBO J*, 22(8):1878–88, 2003. ISSN 0261-4189 (Print) 0261-4189 (Linking). doi: 10.1093/emboj/cdg187. URL `https://www.ncbi.nlm.nih.gov/pubmed/12682020`.

M. F. Jantsch and J. G. Gall. Assembly and localization of the u1-specific snrnp c protein in the amphibian oocyte. *J Cell Biol*, 119(5):1037–46, 1992. ISSN 0021-9525 (Print) 0021-9525 (Linking). doi: 10.1083/jcb.119.5.1037. URL `https://www.ncbi.nlm.nih.gov/pubmed/1447287`.

T. E. Kaiser, R. V. Intine, and M. Dundr. De novo formation of a subnuclear body. *Science*, 322(5908):1713–7, 2008. ISSN 1095-9203 (Electronic) 0036-8075 (Linking). doi: 10.1126/science.1165216. URL `https://www.ncbi.nlm.nih.gov/pubmed/18948503`.

C. Kambach and I. W. Mattaj. Intracellular distribution of the u1a protein depends on active transport and nuclear binding to u1 snrna. *J Cell Biol*, 118 (1):11–21, 1992. ISSN 0021-9525 (Print) 0021-9525 (Linking). doi: 10.1083/ jcb.118.1.11. URL `https://www.ncbi.nlm.nih.gov/pubmed/1618898`.

C. Kambach and I. W. Mattaj. Nuclear transport of the u2 snrnp-specific u2b" protein is mediated by both direct and indirect signalling mechanisms. *J Cell Sci*, 107 (Pt 7):1807–16, 1994. ISSN 0021-9533 (Print) 0021-9533 (Linking). URL `https://www.ncbi.nlm.nih.gov/pubmed/7983149`.

J. Karijolich, A. Kantartzis, and Y. T. Yu. Rna modifications: a mechanism that modulates gene expression. *Methods Mol Biol*, 629:1–19, 2010. ISSN 1940-6029 (Electronic) 1064-3745 (Linking). doi: 10.1007/978-1-60761-657-3_1. URL `https://www.ncbi.nlm.nih.gov/pubmed/20387139`.

Y. Kondo, C. Oubridge, A. M. van Roon, and K. Nagai. Crystal structure of human u1 snrnp, a small nuclear ribonucleoprotein particle, reveals the mechanism of 5' splice site recognition. *Elife*, 4, 2015. ISSN 2050-084X (Electronic) 2050-084X (Linking). doi: 10.7554/eLife.04986. URL `https://www.ncbi.nlm.nih.gov/pubmed/25555158`.

J. P. Kreivi and A. I. Lamond. Rna splicing: unexpected spliceosome diversity. *Curr Biol*, 6(7):802–5, 1996. ISSN 0960-9822 (Print) 0960-9822 (Linking). doi: 10.1016/s0960-9822(02)00599-7. URL `https://www.ncbi.nlm.nih.gov/pubmed/8835860`.

Y. W. Lam, C. E. Lyon, and A. I. Lamond. Large-scale isolation of cajal bodies from hela cells. *Mol Biol Cell*, 13(7):2461–73, 2002. ISSN 1059-1524 (Print) 1059-1524 (Linking). doi: 10.1091/mbc.02-03-0034. URL `https://www.ncbi.nlm.nih.gov/pubmed/12134083`.

R. M. Lardelli and J. Lykke-Andersen. Competition between maturation and degradation drives human snrna 3' end quality control. *Genes Dev*, 34(13-14):989–1001, 2020. ISSN 1549-5477 (Electronic) 0890-9369 (Linking). doi: 10.1101/gad.336891.120. URL `https://www.ncbi.nlm.nih.gov/pubmed/32499401`.

L. Lee, S. E. Davies, and J. L. Liu. The spinal muscular atrophy protein smn affects drosophila germline nuclear organization through the u body-p body pathway. *Dev Biol*, 332(1):142–55, 2009. ISSN 1095-564X (Electronic) 0012-1606 (Linking). doi: 10.1016/j.ydbio.2009.05.553. URL `https://www.ncbi.nlm.nih.gov/pubmed/19464282`.

I. Lemm, C. Girard, A. N. Kuhn, N. J. Watkins, M. Schneider, R. Bordonne, and R. Luhrmann. Ongoing u snrnp biogenesis is required for the integrity of cajal bodies. *Mol Biol Cell*, 17(7):3221–31, 2006. ISSN 1059-1524 (Print) 1059-1524 (Linking). doi: 10.1091/mbc.e06-03-0247. URL `https://www.ncbi.nlm.nih.gov/pubmed/16687569`.

K. Licht, J. Medenbach, R. Luhrmann, C. Kambach, and A. Bindereif. 3'-cyclic phosphorylation of u6 snrna leads to recruitment of recycling factor p110 through lsm proteins. *RNA*, 14(8):1532–8, 2008. ISSN 1469-9001 (Electronic) 1355-8382 (Linking). doi: 10.1261/rna.1129608. URL `https://www.ncbi.nlm.nih.gov/pubmed/18567812`.

J. L. Liu, Z. Wu, Z. Nizami, S. Deryusheva, T. K. Rajendra, K. J. Beumer, H. Gao, A. G. Matera, D. Carroll, and J. G. Gall. Coilin is essential for cajal body organization in drosophila melanogaster. *Mol Biol Cell*, 20(6):1661–70, 2009. ISSN 1939-4586 (Electronic) 1059-1524 (Linking). doi: 10.1091/mbc.E08-05-0525. URL `https://www.ncbi.nlm.nih.gov/pubmed/19158395`.

S. Liu, R. Rauhut, H. P. Vornlocher, and R. Luhrmann. The network of protein-protein interactions within the human u4/u6.u5 tri-snrnp. *RNA*, 12(7):1418–30, 2006. ISSN 1355-8382 (Print) 1355-8382 (Linking). doi: 10.1261/rna.55406. URL `https://www.ncbi.nlm.nih.gov/pubmed/16723661`.

C. L. Lorson, J. Strasswimmer, J. M. Yao, J. D. Baleja, E. Hahnen, B. Wirth, T. Le, A. H. Burghes, and E. J. Androphy. Smn oligomerization defect correlates with spinal muscular atrophy severity. *Nat Genet*, 19(1):63–6, 1998. ISSN 1061-4036 (Print) 1061-4036 (Linking). doi: 10.1038/ng0598-63. URL `https://www.ncbi.nlm.nih.gov/pubmed/9590291`.

E. Lund and J. E. Dahlberg. Cyclic 2',3'-phosphates and nontemplated nucleotides at the 3' end of spliceosomal u6 small nuclear rna's. *Science*, 255(5042):327–30, 1992. ISSN 0036-8075 (Print) 0036-8075 (Linking). doi: 10.1126/science.1549778. URL `https://www.ncbi.nlm.nih.gov/pubmed/1549778`.

M. Machyna, S. Kehr, K. Straube, D. Kappei, F. Buchholz, F. Butter, J. Ule, J. Hertel, P. F. Stadler, and K. M. Neugebauer. The coilin interactome identifies hundreds of small noncoding rnas that traffic through cajal bodies. *Mol Cell*, 56(3):389–399, 2014. ISSN 1097-4164 (Electronic) 1097-2765 (Linking). doi: 10.1016/j.molcel.2014.10.004. URL `https://www.ncbi.nlm.nih.gov/pubmed/25514182`.

M. Machyna, K. M. Neugebauer, and D. Stanek. Coilin: The first 25 years. *RNA Biol*, 12(6):590–6, 2015. ISSN 1555-8584 (Electronic) 1547-6286 (Linking). doi: 10.1080/15476286.2015.1034923. URL `https://www.ncbi.nlm.nih.gov/pubmed/25970135`.

E. M. Makarov, O. V. Makarova, T. Achsel, and R. Luhrmann. The human homologue of the yeast splicing factor prp6p contains multiple tpr elements and is stably associated with the u5 snrnp via protein-protein interactions. *J Mol Biol*, 298(4):567–75, 2000. ISSN 0022-2836 (Print) 0022-2836 (Linking). doi: 10.1006/jmbi.2000.3685. URL `https://www.ncbi.nlm.nih.gov/pubmed/10788320`.

O. V. Makarova, E. M. Makarov, S. Liu, H. P. Vornlocher, and R. Luhrmann. Protein 61k, encoded by a gene (prpf31) linked to autosomal dominant retinitis pigmentosa, is required for u4/u6*u5 tri-snrnp formation and pre-mrna splicing. *EMBO J*, 21(5):1148–57, 2002. ISSN 0261-4189 (Print) 0261-4189 (Linking). doi: 10.1093/emboj/21.5.1148. URL `https://www.ncbi.nlm.nih.gov/pubmed/11867543`.

T. Masek, V. Vopalensky, P. Suchomelova, and M. Pospisek. Denaturing rna electrophoresis in tae agarose gels. *Anal Biochem*, 336(1):46–50, 2005. ISSN 0003-2697 (Print) 0003-2697 (Linking). doi: 10.1016/j.ab.2004.09.010. URL `https://www.ncbi.nlm.nih.gov/pubmed/15582557`.

A. G. Matera and K. B. Shpargel. Pumping rna: nuclear bodybuilding along the rnp pipeline. *Curr Opin Cell Biol*, 18(3):317–24, 2006. ISSN 0955-0674 (Print) 0955-0674 (Linking). doi: 10.1016/j.ceb.2006.03.005. URL `https://www.ncbi.nlm.nih.gov/pubmed/16632338`.

A. G. Matera and Z. Wang. A day in the life of the spliceosome. *Nat Rev Mol Cell Biol*, 15(2):108–21, 2014. ISSN 1471-0080 (Electronic) 1471-0072 (Linking). doi: 10.1038/nrm3742. URL `https://www.ncbi.nlm.nih.gov/pubmed/24452469`.

A. G. Matera, R. M. Terns, and M. P. Terns. Non-coding rnas: lessons from the small nuclear and small nucleolar rnas. *Nat Rev Mol Cell Biol*, 8(3):209–20, 2007. ISSN 1471-0072 (Print) 1471-0072 (Linking). doi: 10.1038/nrm2124. URL `https://www.ncbi.nlm.nih.gov/pubmed/17318225`.

G. Meister and U. Fischer. Assisted rnp assembly: Smn and prmt5 complexes cooperate in the formation of spliceosomal usnrnps. *EMBO J*, 21(21):5853–63, 2002. ISSN 0261-4189 (Print) 0261-4189 (Linking). doi: 10.1093/emboj/cdf585. URL `https://www.ncbi.nlm.nih.gov/pubmed/12411503`.

G. Meister, D. Buhler, R. Pillai, F. Lottspeich, and U. Fischer. A multiprotein complex mediates the atp-dependent assembly of spliceosomal u snrnps. *Nat Cell Biol*, 3(11):945–9, 2001a. ISSN 1465-7392 (Print) 1465-7392 (Linking). doi: 10.1038/ncb1101-945. URL `https://www.ncbi.nlm.nih.gov/pubmed/11715014`.

G. Meister, C. Eggert, D. Buhler, H. Brahms, C. Kambach, and U. Fischer. Methylation of sm proteins by a complex containing prmt5 and the putative u snrnp assembly factor picln. *Curr Biol*, 11(24):1990–4, 2001b. ISSN 0960-9822 (Print) 0960-9822 (Linking). doi: 10.1016/s0960-9822(01)00592-9. URL `https://www.ncbi.nlm.nih.gov/pubmed/11747828`.

J. Mouaikel, C. Verheggen, E. Bertrand, J. Tazi, and R. Bordonne. Hypermethylation of the cap structure of both yeast snrnas and snornas requires a conserved methyltransferase that is localized to the nucleolus. *Mol Cell*, 9(4):891–901, 2002. ISSN 1097-2765 (Print) 1097-2765 (Linking). doi: 10.1016/s1097-2765(02)00484-7. URL https://www.ncbi.nlm.nih.gov/pubmed/11983179.

U. Narayanan, J. K. Ospina, M. R. Frey, M. D. Hebert, and A. G. Matera. Smn, the spinal muscular atrophy protein, forms a pre-import snrnp complex with snurportin1 and importin beta. *Hum Mol Genet*, 11(15):1785–95, 2002. ISSN 0964-6906 (Print) 0964-6906 (Linking). doi: 10.1093/hmg/11.15.1785. URL https://www.ncbi.nlm.nih.gov/pubmed/12095920.

D. Nesic, G. Tanackovic, and A. Kramer. A role for cajal bodies in the final steps of u2 snrnp biogenesis. *J Cell Sci*, 117(Pt 19):4423–33, 2004. ISSN 0021-9533 (Print) 0021-9533 (Linking). doi: 10.1242/jcs.01308. URL https://www.ncbi.nlm.nih.gov/pubmed/15316075.

T. H. Nguyen, W. P. Galej, X. C. Bai, C. G. Savva, A. J. Newman, S. H. Scheres, and K. Nagai. The architecture of the spliceosomal u4/u6.u5 tri-snrnp. *Nature*, 523(7558):47–52, 2015. ISSN 1476-4687 (Electronic) 0028-0836 (Linking). doi: 10.1038/nature14548. URL https://www.ncbi.nlm.nih.gov/pubmed/26106855.

S. Nielsen, Y. Yuzenkova, and N. Zenkin. Mechanism of eukaryotic rna polymerase iii transcription termination. *Science*, 340(6140):1577–80, 2013. ISSN 1095-9203 (Electronic) 0036-8075 (Linking). doi: 10.1126/science.1237934. URL https://www.ncbi.nlm.nih.gov/pubmed/23812715.

S. Nottrott, H. Urlaub, and R. Luhrmann. Hierarchical, clustered protein interactions with u4/u6 snrna: a biochemical role for u4/u6 proteins. *EMBO J*, 21 (20):5527–38, 2002. ISSN 0261-4189 (Print) 0261-4189 (Linking). doi: 10.1093/emboj/cdf544. URL https://www.ncbi.nlm.nih.gov/pubmed/12374753.

I. Novotny, M. Blazikova, D. Stanek, P. Herman, and J. Malinsky. In vivo kinetics of u4/u6.u5 tri-snrnp formation in cajal bodies. *Mol Biol Cell*, 22(4):513–23, 2011. ISSN 1939-4586 (Electronic) 1059-1524 (Linking). doi: 10.1091/mbc.E10-07-0560. URL https://www.ncbi.nlm.nih.gov/pubmed/21177826.

I. Novotny, A. Malinova, E. Stejskalova, D. Mateju, K. Klimesova, A. Roithova, M. Sveda, Z. Knejzlik, and D. Stanek. Sart3-dependent accumulation of incomplete spliceosomal snrnps in cajal bodies. *Cell Rep*, 10(3):429–440, 2015. ISSN 2211-1247 (Electronic). doi: 10.1016/j.celrep.2014.12.030. URL https://www.ncbi.nlm.nih.gov/pubmed/25600876.

M. Ohno, A. Segref, A. Bachi, M. Wilm, and I. W. Mattaj. Phax, a mediator of u snrna nuclear export whose activity is regulated by phosphorylation. *Cell*, 101(2):187–98, 2000. ISSN 0092-8674 (Print) 0092-8674 (Linking). doi: 10.1016/S0092-8674(00)80829-6. URL https://www.ncbi.nlm.nih.gov/pubmed/10786834.

I. Palacios, M. Hetzer, S. A. Adam, and I. W. Mattaj. Nuclear import of u snrnps requires importin beta. *EMBO J*, 16(22):6783–92, 1997. ISSN 0261-4189 (Print) 0261-4189 (Linking). doi: 10.1093/emboj/16.22.6783. URL `https://www.ncbi.nlm.nih.gov/pubmed/9362492`.

C. Plaschka, P. C. Lin, and K. Nagai. Structure of a pre-catalytic spliceosome. *Nature*, 546(7660):617–621, 2017. ISSN 1476-4687 (Electronic) 0028-0836 (Linking). doi: 10.1038/nature22799. URL `https://www.ncbi.nlm.nih.gov/pubmed/28530653`.

D. A. Pomeranz Krummel, C. Oubridge, A. K. Leung, J. Li, and K. Nagai. Crystal structure of human spliceosomal u1 snrnp at 5.5 a resolution. *Nature*, 458 (7237):475–80, 2009. ISSN 1476-4687 (Electronic) 0028-0836 (Linking). doi: 10.1038/nature07851. URL `https://www.ncbi.nlm.nih.gov/pubmed/19325628`.

O. Puig, E. Bragado-Nilsson, T. Koski, and B. Seraphin. The u1 snrnp-associated factor luc7p affects 5' splice site selection in yeast and human. *Nucleic Acids Res*, 35(17):5874–85, 2007. ISSN 1362-4962 (Electronic) 0305-1048 (Linking). doi: 10.1093/nar/gkm505. URL `https://www.ncbi.nlm.nih.gov/pubmed/17726058`.

P. L. Raghunathan and C. Guthrie. Rna unwinding in u4/u6 snrnps requires atp hydrolysis and the deih-box splicing factor brr2. *Curr Biol*, 8(15):847–55, 1998. ISSN 0960-9822 (Print) 0960-9822 (Linking). doi: 10.1016/s0960-9822(07) 00345-4. URL `https://www.ncbi.nlm.nih.gov/pubmed/9705931`.

I. Raska, L. E. Andrade, R. L. Ochs, E. K. Chan, C. M. Chang, G. Roos, and E. M. Tan. Immunological and ultrastructural studies of the nuclear coiled body with autoimmune antibodies. *Exp Cell Res*, 195(1):27–37, 1991. ISSN 0014-4827 (Print) 0014-4827 (Linking). doi: 10.1016/0014-4827(91)90496-h. URL `https://www.ncbi.nlm.nih.gov/pubmed/2055273`.

R. Reddy. Transcription of a u6 small nuclear rna gene in vitro. transcription of a mouse u6 small nuclear rna gene in vitro by rna polymerase iii is dependent on transcription factor(s) different from transcription factors iiia, iiib, and iiic. *J Biol Chem*, 263(31):15980–4, 1988. ISSN 0021-9258 (Print) 0021-9258 (Linking). URL `https://www.ncbi.nlm.nih.gov/pubmed/3182777`.

Ram Reddy and Harris Busch. *Small Nuclear RNAs: RNA Sequences, Structure, and Modifications*, pages 1–37. Springer Berlin Heidelberg, Berlin, Heidelberg, 1988. ISBN 978-3-642-73020-7. doi: 10.1007/978-3-642-73020-7_1. URL `https://doi.org/10.1007/978-3-642-73020-7_1`.

J. Rinke and J. A. Steitz. Association of the lupus antigen la with a subset of u6 snrna molecules. *Nucleic Acids Res*, 13(7):2617–29, 1985. ISSN 0305-1048 (Print) 0305-1048 (Linking). doi: 10.1093/nar/13.7.2617. URL `https://www.ncbi.nlm.nih.gov/pubmed/2582364`.

T. L. Riss, R. A. Moravec, A. L. Niles, S. Duellman, H. A. Benink, T. J. Worzella, and L. Minor. *Cell Viability Assays*. Bethesda (MD), 2004. URL `https://www.ncbi.nlm.nih.gov/pubmed/23805433`.

A. Roithova, K. Klimesova, J. Panek, C. L. Will, R. Luhrmann, D. Stanek, and C. Girard. The sm-core mediates the retention of partially-assembled spliceosomal snrnps in cajal bodies until their full maturation. *Nucleic Acids Res*, 46(7): 3774–3790, 2018. ISSN 1362-4962 (Electronic) 0305-1048 (Linking). doi: 10. 1093/nar/gky070. URL `https://www.ncbi.nlm.nih.gov/pubmed/29415178`.

A. Roithova, Z. Feketova, S. Vanacova, and D. Stanek. Dis3l2 and lsm proteins are involved in the surveillance of sm ring-deficient snrnas. *Nucleic Acids Res*, 48(11):6184–6197, 2020. ISSN 1362-4962 (Electronic) 0305-1048 (Linking). doi: 10.1093/nar/gkaa301. URL `https://www.ncbi.nlm.nih.gov/pubmed/32374871`.

J. M. Romac, D. H. Graff, and J. D. Keene. The u1 small nuclear ribonucleoprotein (snrnp) 70k protein is transported independently of u1 snrnp particles via a nuclear localization signal in the rna-binding domain. *Mol Cell Biol*, 14(7):4662–70, 1994. ISSN 0270-7306 (Print) 0270-7306 (Linking). doi: 10.1128/mcb.14.7.4662-4670.1994. URL `https://www.ncbi.nlm.nih.gov/pubmed/7516470`.

M. Sanz-Garcia, M. Vazquez-Cedeira, E. Kellerman, P. Renbaum, E. Levy-Lahad, and P. A. Lazo. Substrate profiling of human vaccinia-related kinases identifies coilin, a cajal body nuclear protein, as a phosphorylation target with neurological implications. *J Proteomics*, 75(2):548–60, 2011. ISSN 1876-7737 (Electronic) 1874-3919 (Linking). doi: 10.1016/j.jprot.2011.08.019. URL `https://www.ncbi.nlm.nih.gov/pubmed/21920476`.

N. Schaffert, M. Hossbach, R. Heintzmann, T. Achsel, and R. Luhrmann. Rnai knockdown of hprp31 leads to an accumulation of u4/u6 di-snrnps in cajal bodies. *EMBO J*, 23(15):3000–9, 2004. ISSN 0261-4189 (Print) 0261-4189 (Linking). doi: 10.1038/sj.emboj.7600296. URL `https://www.ncbi.nlm.nih.gov/pubmed/15257298`.

J. Schindelin, I. Arganda-Carreras, E. Frise, V. Kaynig, M. Longair, T. Pietzsch, S. Preibisch, C. Rueden, S. Saalfeld, B. Schmid, J. Y. Tinevez, D. J. White, V. Hartenstein, K. Eliceiri, P. Tomancak, and A. Cardona. Fiji: an open-source platform for biological-image analysis. *Nat Methods*, 9(7):676–82, 2012. ISSN 1548-7105 (Electronic) 1548-7091 (Linking). doi: 10.1038/nmeth.2019. URL `https://www.ncbi.nlm.nih.gov/pubmed/22743772`.

D. G. Scofield and M. Lynch. Evolutionary diversification of the sm family of rna-associated proteins. *Mol Biol Evol*, 25(11):2255–67, 2008. ISSN 1537-1719 (Electronic) 0737-4038 (Linking). doi: 10.1093/molbev/msn175. URL `https://www.ncbi.nlm.nih.gov/pubmed/18687770`.

R. Shanbhag, A. Kurabi, J. J. Kwan, and L. W. Donaldson. Solution structure of the carboxy-terminal tudor domain from human coilin. *FEBS Lett*, 584(20):4351–6, 2010. ISSN 1873-3468 (Electronic) 0014-5793 (Linking). doi: 10.1016/j.febslet.2010.09.034. URL `https://www.ncbi.nlm.nih.gov/pubmed/20875822`.

Y. Shi. The spliceosome: A protein-directed metalloribozyme. *J Mol Biol*, 429 (17):2640–2653, 2017. ISSN 1089-8638 (Electronic) 0022-2836 (Linking). doi: 10.1016/j.jmb.2017.07.010. URL `https://www.ncbi.nlm.nih.gov/pubmed/28733144`.

R. Singh and R. Reddy. Gamma-monomethyl phosphate: a cap structure in spliceosomal u6 small nuclear rna. *Proc Natl Acad Sci U S A*, 86(21):8280–3, 1989. ISSN 0027-8424 (Print) 0027-8424 (Linking). doi: 10.1073/pnas.86.21.8280. URL `https://www.ncbi.nlm.nih.gov/pubmed/2813391`.

J. E. Sleeman and A. I. Lamond. Newly assembled snrnps associate with coiled bodies before speckles, suggesting a nuclear snrnp maturation pathway. *Curr Biol*, 9(19):1065–74, 1999. ISSN 0960-9822 (Print) 0960-9822 (Linking). doi: 10.1016/s0960-9822(99)80475-8. URL `https://www.ncbi.nlm.nih.gov/pubmed/10531003`.

E. C. Small, S. R. Leggett, A. A. Winans, and J. P. Staley. The ef-g-like gtpase snu114p regulates spliceosome dynamics mediated by brr2p, a dexd/h box atpase. *Mol Cell*, 23(3):389–99, 2006. ISSN 1097-2765 (Print) 1097-2765 (Linking). doi: 10.1016/j.molcel.2006.05.043. URL `https://www.ncbi.nlm.nih.gov/pubmed/16885028`.

K. P. Smith, K. C. Carter, C. V. Johnson, and J. B. Lawrence. U2 and u1 snrna gene loci associate with coiled bodies. *J Cell Biochem*, 59(4):473–85, 1995. ISSN 0730-2312 (Print) 0730-2312 (Linking). doi: 10.1002/jcb.240590408. URL `https://www.ncbi.nlm.nih.gov/pubmed/8749717`.

D. L. Spector, G. Lark, and S. Huang. Differences in snrnp localization between transformed and nontransformed cells. *Mol Biol Cell*, 3(5):555–69, 1992. ISSN 1059-1524 (Print) 1059-1524 (Linking). doi: 10.1091/mbc.3.5.555. URL `https://www.ncbi.nlm.nih.gov/pubmed/1535243`.

D. Stanek and K. M. Neugebauer. Detection of snrnp assembly intermediates in cajal bodies by fluorescence resonance energy transfer. *J Cell Biol*, 166(7): 1015–25, 2004. ISSN 0021-9525 (Print) 0021-9525 (Linking). doi: 10.1083/jcb.200405160. URL `https://www.ncbi.nlm.nih.gov/pubmed/15452143`.

D. Stanek, S. D. Rader, M. Klingauf, and K. M. Neugebauer. Targeting of u4/u6 small nuclear rnp assembly factor sart3/p110 to cajal bodies. *J Cell Biol*, 160 (4):505–16, 2003. ISSN 0021-9525 (Print) 0021-9525 (Linking). doi: 10.1083/jcb.200210087. URL `https://www.ncbi.nlm.nih.gov/pubmed/12578909`.

M. Strzelecka, S. Trowitzsch, G. Weber, R. Luhrmann, A. C. Oates, and K. M. Neugebauer. Coilin-dependent snrnp assembly is essential for zebrafish embryogenesis. *Nat Struct Mol Biol*, 17(4):403–9, 2010. ISSN 1545-9985 (Electronic) 1545-9985 (Linking). doi: 10.1038/nsmb.1783. URL `https://www.ncbi.nlm.nih.gov/pubmed/20357773`.

T. Suzuki, H. Izumi, and M. Ohno. Cajal body surveillance of u snrna export complex assembly. *J Cell Biol*, 190(4):603–12, 2010. ISSN 1540-8140 (Electronic) 0021-9525 (Linking). doi: 10.1083/jcb.201004109. URL `https://www.ncbi.nlm.nih.gov/pubmed/20733056`.

H. Takata, H. Nishijima, K. Maeshima, and K. Shibahara. The integrator complex is required for integrity of cajal bodies. *J Cell Sci*, 125(Pt 1):166–75, 2012. ISSN 1477-9137 (Electronic) 0021-9533 (Linking). doi: 10.1242/jcs.090837. URL https://www.ncbi.nlm.nih.gov/pubmed/22250197.

G. Tanackovic and A. Kramer. Human splicing factor sf3a, but not sf1, is essential for pre-mrna splicing in vivo. *Mol Biol Cell*, 16(3):1366–77, 2005. ISSN 1059-1524 (Print) 1059-1524 (Linking). doi: 10.1091/mbc.e04-11-1034. URL https://www.ncbi.nlm.nih.gov/pubmed/15647371.

P. J. Thul, L. Akesson, M. Wiking, D. Mahdessian, A. Geladaki, H. Ait Blal, T. Alm, A. Asplund, L. Bjork, L. M. Breckels, A. Backstrom, F. Danielsson, L. Fagerberg, J. Fall, L. Gatto, C. Gnann, S. Hober, M. Hjelmare, F. Johansson, S. Lee, C. Lindskog, J. Mulder, C. M. Mulvey, P. Nilsson, P. Oksvold, J. Rockberg, R. Schutten, J. M. Schwenk, A. Sivertsson, E. Sjostedt, M. Skogs, C. Stadler, D. P. Sullivan, H. Tegel, C. Winsnes, C. Zhang, M. Zwahlen, A. Mardinoglu, F. Ponten, K. von Feilitzen, K. S. Lilley, M. Uhlen, and E. Lundberg. A subcellular map of the human proteome. *Science*, 356(6340), 2017. ISSN 1095-9203 (Electronic) 0036-8075 (Linking). doi: 10.1126/science.aal3321. URL https://www.ncbi.nlm.nih.gov/pubmed/28495876.

R. Trippe, E. Guschina, M. Hossbach, H. Urlaub, R. Luhrmann, and B. J. Benecke. Identification, cloning, and functional analysis of the human u6 snrna-specific terminal uridylyl transferase. *RNA*, 12(8):1494–504, 2006. ISSN 1355-8382 (Print) 1355-8382 (Linking). doi: 10.1261/rna.87706. URL https://www.ncbi.nlm.nih.gov/pubmed/16790842.

K. E. Tucker, M. T. Berciano, E. Y. Jacobs, D. F. LePage, K. B. Shpargel, J. J. Rossire, E. K. Chan, M. Lafarga, R. A. Conlon, and A. G. Matera. Residual cajal bodies in coilin knockout mice fail to recruit sm snrnps and smn, the spinal muscular atrophy gene product. *J Cell Biol*, 154(2):293–307, 2001. ISSN 0021-9525 (Print) 0021-9525 (Linking). doi: 10.1083/jcb.200104083. URL https://www.ncbi.nlm.nih.gov/pubmed/11470819.

Z. Wang and C. B. Burge. Splicing regulation: from a parts list of regulatory elements to an integrated splicing code. *RNA*, 14(5):802–13, 2008. ISSN 1469-9001 (Electronic) 1355-8382 (Linking). doi: 10.1261/rna.876308. URL https://www.ncbi.nlm.nih.gov/pubmed/18369186.

A. A. Whittom, H. Xu, and M. D. Hebert. Coilin levels and modifications influence artificial reporter splicing. *Cell Mol Life Sci*, 65(7-8):1256–71, 2008. ISSN 1420-682X (Print) 1420-682X (Linking). doi: 10.1007/s00018-008-7587-3. URL https://www.ncbi.nlm.nih.gov/pubmed/18322647.

M. E. Wilkinson, C. Charenton, and K. Nagai. Rna splicing by the spliceosome. *Annu Rev Biochem*, 89:359–388, 2020. ISSN 1545-4509 (Electronic) 0066-4154 (Linking). doi: 10.1146/annurev-biochem-091719-064225. URL https://www.ncbi.nlm.nih.gov/pubmed/31794245.

D. Wohlwend, A. Strasser, A. Dickmanns, and R. Ficner. Structural basis for rangtp independent entry of spliceosomal u snrnps into the nucleus. *J Mol*

Biol, 374(4):1129–38, 2007. ISSN 1089-8638 (Electronic) 0022-2836 (Linking). doi: 10.1016/j.jmb.2007.09.065. URL `https://www.ncbi.nlm.nih.gov/pubmed/18028944`.

H. Xu and M. D. Hebert. A novel eb-1/aida-1 isoform, aida-1c, interacts with the cajal body protein coilin. *BMC Cell Biol*, 6(1):23, 2005. ISSN 1471-2121 (Electronic) 1471-2121 (Linking). doi: 10.1186/1471-2121-6-23. URL `https://www.ncbi.nlm.nih.gov/pubmed/15862129`.

H. Xu, R. S. Pillai, T. N. Azzouz, K. B. Shpargel, C. Kambach, M. D. Hebert, D. Schumperli, and A. G. Matera. The c-terminal domain of coilin interacts with sm proteins and u snrnps. *Chromosoma*, 114(3):155–66, 2005. ISSN 0009-5915 (Print) 0009-5915 (Linking). doi: 10.1007/s00412-005-0003-y. URL `https://www.ncbi.nlm.nih.gov/pubmed/16003501`.

J. Yong, M. Kasim, J. L. Bachorik, L. Wan, and G. Dreyfuss. Gemin5 delivers snrna precursors to the smn complex for snrnp biogenesis. *Mol Cell*, 38(4):551–62, 2010. ISSN 1097-4164 (Electronic) 1097-2765 (Linking). doi: 10.1016/j.molcel.2010.03.014. URL `https://www.ncbi.nlm.nih.gov/pubmed/20513430`.

Y. T. Yu, M. D. Shu, and J. A. Steitz. Modifications of u2 snrna are required for snrnp assembly and pre-mrna splicing. *EMBO J*, 17(19):5783–95, 1998. ISSN 0261-4189 (Print) 0261-4189 (Linking). doi: 10.1093/emboj/17.19.5783. URL `https://www.ncbi.nlm.nih.gov/pubmed/9755178`.

Z. Zhang, C. L. Will, K. Bertram, O. Dybkov, K. Hartmuth, D. E. Agafonov, R. Hofele, H. Urlaub, B. Kastner, R. Luhrmann, and H. Stark. Molecular architecture of the human 17s u2 snrnp. *Nature*, 583(7815):310–313, 2020. ISSN 1476-4687 (Electronic) 0028-0836 (Linking). doi: 10.1038/s41586-020-2344-3. URL `https://www.ncbi.nlm.nih.gov/pubmed/32494006`.

L. Zhou, J. Hang, Y. Zhou, R. Wan, G. Lu, P. Yin, C. Yan, and Y. Shi. Crystal structures of the lsm complex bound to the 3' end sequence of u6 small nuclear rna. *Nature*, 506(7486):116–20, 2014. ISSN 1476-4687 (Electronic) 0028-0836 (Linking). doi: 10.1038/nature12803. URL `https://www.ncbi.nlm.nih.gov/pubmed/24240276`.

List of Figures

List of Tables